Inorg. Chem. **2003**, *42*, 6749–6763

Nickel(II) Cyclidenes with Appended Ethylpyridine Receptor Centers as Molecular Tweezers for Dicarboxylic Acids

Jeremy S. Disch,[†] Richard J. Staples,[‡] Thomas E. Concolino,[§] Terry E. Haas,[†] and Elena V. Rybak-Akimova*,[†]

Department of Chemistry, Tufts University, Medford, Massachusetts 02155, Department of Chemistry and Chemical Biology, Harvard University, Cambridge, Massachusetts 02138, and Rigaku MSC, 9009 New Trails Drive, The Woodlands, Texas 77381

Received May 23, 2003

A series of 14-, 15-, and 16-membered nickel(II) cyclidene macrocycles appended with 2-aminoethyl(2-pyridine) receptors **I**–**III**, respectively, were prepared and characterized by X-ray crystallography and NMR techniques. The 14- and 15-membered macrocycles **I** and **II** exist in a planar or extended Z-configuration, whereas the 16-membered macrocycle **III** was saddle shaped and had two asymmetric configurations in the unit cell (**IIIa** in a "capped" configuration and **IIIb** in an "open" configuration). Variable-temperature ^{1}H NMR studies of **III** in CD_3CN were conducted (25–65 °C), and at room temperature, the interconversion between capping and uncapping is slow on the NMR time scale, resulting in a broad spectrum, whereas at 65 °C, interconversion was fast. ^{1}H NMR binding studies indicated **I**–**III** bind unsaturated dicarboxylic acids in a 1:1 stoichiometry with binding constants approaching 400 M^{-1} in CD_3CN, and the binding strength was dependent on the shape of the macrocyclic cyclidene platforms, whereas monocarboxylic acids were not bound. Generally, the planar 14-membered cyclidene **I** bound diacids the weakest and the 16-membered cyclidene **III** bound diacids the strongest. The presence of nuclear Overhauser effect spectrometry cross peaks in a 20 mM solution of 1:1 **II**–maleic acid indicates that the binding mode is ditopic with the guest being encapsulated by the aminoethylpyridine arms above the macrocyclic framework.

Introduction

Multipoint recognition of organic molecules and ions is an efficient way of designing size- and shape-selective receptors with high affinity for substrates.[1−3] Unlike metal cations, neutral molecules or anions ordinarily do not form strong coordination bonds with their "ligands" (receptors), thus multiple interactions between the substrate and the receptor are needed for their efficient recognition.[2,4] Dicarboxylic acids and their anions remain among the most attractive targets for molecular recognition[5−36] since the presence of several carboxylate functional groups is typical for a variety of biomolecules, ranging from simple aliphatic di- and tricarboxylic acids involved in the citric acid cycle to amino acids and proteins.

* To whom correspondence should be addressed. E-mail: elena.rybak-akimova@tufts.edu. Fax: 617-627-3443. Tel: 617-627-3413.
[†] Tufts University.
[‡] Harvard University.
[§] Rigaku MSC.

(1) Lehn, J.-M. *Supramolecular chemistry: concepts and perspectives*; VCH: New York, 1995.
(2) *Supramolecular Chemistry of Anions*; Bianchi, A., Bowman-James, K., Garcia-Espana, E., Eds.; Wiley-VCH: New York, 1997.
(3) Hartley, J. H.; James, T. D.; Ward, C. J. *J. Chem. Soc., Perkin Trans. 1* **2000**, 3155−3184.
(4) Gale, P. A. *Coord. Chem. Rev.* **2000**, *199*, 181−233.
(5) Fitzmaurice, R. J.; Kyne, G. M.; Douheret, D.; Kilburn, J. D. *J. Chem. Soc., Perkin Trans. 1* **2002**, 841−864.
(6) Raker, J.; Glass, T. E. *J. Org. Chem.* **2002**, *67*, 6113−6116.
(7) Rossi, S.; Kyne, G. M.; Turner, D. L.; Wells, N. J.; Kilburn, J. D. *Angew. Chem., Int. Ed.* **2002**, *41*, 4233−4236.
(8) Sansenon, F.; Martinez-Manez, R.; Miranda, M. A.; Segui, M.-J.; Soto, J. *Angew. Chem., Int. Ed.* **2003**, *42*, 647−650.
(9) Miyaji, H.; Dudic, M.; Tucker, J. H. R.; Prokes, I.; Light, M. E.; Hursthouse, M. B.; Stibor, I.; Lhotak, P. *Tetrahedron Lett.* **2002**, *43*, 873−878.
(10) Ishi-i, T.; Grego-Calama, M.; Timmerman, P.; Reinhoudt, D. N.; Shinkai, S. *Angew. Chem., Int. Ed.* **2002**, *41*, 1924−1929.
(11) Seel, C.; Galan, A.; de Mendoza, J. *Top. Curr. Chem.* **1995**, *175*, 101−132.
(12) Benito, H. M.; Gomez-Garcia, M.; Jimenez Blanco, J. L.; Mellet, C. O.; Garcia Fernandez, J. M. *J. Org. Chem.* **2001**, *66*, 1366−1372.
(13) Mei, M.; Wu, S. *New J. Chem.* **2001**, *25*, 471−475.
(14) Carr, J. D.; Coles, S. J.; Hursthouse, M. B.; Light, M. E.; Tucker, J. H. R.; Westwood, J. *Angew. Chem., Int. Ed.* **2000**, *39*, 3296−3299.
(15) Watanabe, S.; Higashi, N.; Kobayashi, M.; Hamanaka, K.; Takata, Y.; Yoshida, K. *Tetrahedron Lett.* **2000**, *41*, 4583−4586.
(16) Alfonso, I.; Rebolledo, F.; Gotor, V. *Chem.−Eur. J.* **2000**, *6*, 3331−3338.
(17) Ahn, D.-R.; Kim, T. W.; Hong, J. I. *Tetrahedron Lett.* **1999**, *40*, 6045−6048.

10.1021/ic0345572 CCC: $25.00
Published on Web 09/20/2003

One of the challenges in designing ditopic receptors for dicarboxylic acids is to accomplish shape complementarity between the functional groups in the guest and the binding sites in the host. This is often achieved by attaching two (or more) receptor sites (e.g., polyamines, amidinium or guanidinium fragments, amidopyridines, etc., that are capable of electrostatic and hydrogen bonding interactions with carboxylates)[5] to a rigid molecular scaffold.

It is desirable to incorporate metal ions into multicenter receptors because the metal ions can act as additional binding sites, as reactive centers, or as indicators of guest binding.[37−40] Metal ions were shown to play several advantageous roles in designing dicarboxylate receptors: (1) self-assembly of polyfunctional receptors was accomplished via coordination of several receptor fragments to the metal ions;[15,31,32,41,42] (2) direct coordination to the metal centers was used for carboxylate binding;[29,43−48] (3) binding affinities were increased due to favorable electrostatic interactions between positively charged metal centers in the hosts and the anionic guests;[14,49−51] and (4) metals served as redox,[14,49,50,52] fluorescent,[15] or colorimetric[42] reporters of carboxylate binding events.

Scheme 1. Synthesis of **I**−**III** for Structures **I** (x, y = 0; R_1, R_3 = CH_3; R_2 = H), **II** (x = 0; y = 1; R_1, R_2 = CH'_3; R_3 = H), and **III** (x, y = 1; R_1, R_2 = CH_3; R_3 = H)

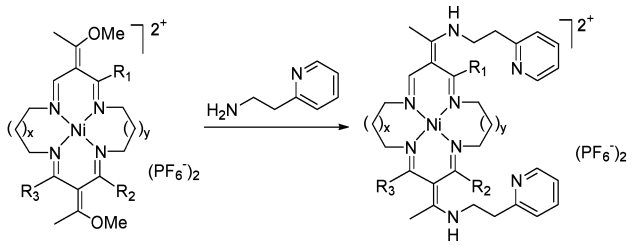

We present the preparation of ditopic receptors for dicarboxylic acids based on a metal-containing macrocyclic cleft. In this design, the metal ion is incorporated into the macrocyclic platform with high affinity, so that no loss of the metal is expected during the recognition process. Cyclidene macrocycles (Scheme 1)[53] were selected as scaffolds for the clefts. The distinctive features of the cyclidene scaffold include the relative flexibility of the cleft,[53−56] which, in principle, allows for the regulation of the substrate binding affinity and selectivity via conformational changes in the platform and the positioning of the guest right above the metal center, thus suggesting potential involvement of the metal in the catalytic regioselective transformations of the substrates. Examples of regioselective reagents and catalysts based on functionalized rigid metalloporphyrins were provided by Breslow[57−63] and Woggon.[64−66] Unlike porphyrins, the cyclidene platform can adopt both "open" (planar) and "closed" (saddle-shaped) conformations.[53,54] This dual-shape feature is needed in order to eventually obtain switchable

(18) Hossain, M. A.; Schneider, H.-J. *Chem.−Eur. J.* **1999**, *5*, 1284−1290.
(19) Jeong, K.-S.; Park, J. W.; Cho, Y. L. *Tetrahedron Lett.* **1996**, *37*, 2795−2798.
(20) Cudic, P.; Vigneron, J.-P.; Lehn, J.-M.; Cesario, M.; Prange, T. *Eur. J. Org. Chem.* **1999**, *10*, 2479−2484.
(21) Teulade-Fichou, M.-P.; Vigneron, J.-P.; Lehn, J.-M. *J. Chem. Soc., Perkin Trans. 2* **1996**, 2169−2175.
(22) Sebo, L.; Diedrich, F.; Gramlich, V. *Helv. Chim. Acta* **2000**, *83*, 93−113.
(23) Sebo, L.; Schweiger, B.; Diedrich, F. *Helv. Chim. Acta* **2000**, *83*, 80−92.
(24) Lustenberger, P.; Welti, R.; Diedrich, F. *Helv. Chim. Acta* **1998**, *81*, 2190−2200.
(25) Lustenberger, P.; Martinborough, E.; Denti, T. M.; Diedrich, F. *J. Chem. Soc., Perkin Trans. 2* **1998**, 747−761.
(26) Hinzen, B.; Seiler, P.; Diedrich, F. *Helv. Chim. Acta* **1996**, *79*, 942−960.
(27) Shao, Y.; Linton, B.; Hamilton, A. D.; Weber, S. G. *J. Electroanal. Chem.* **1998**, *441*, 33−37.
(28) Sessler, J. L.; Andrievsky, A.; Kral, V.; Lynch, V. *J. Am. Chem. Soc.* **1997**, *119*, 9385−9392.
(29) Bazzicalupi, C.; Bencini, A.; Bianchi, A.; Fusi, V.; Garcia-Espana, E.; Giorgi, C.; Llinares, J. M.; Ramirez, J. A.; Valtancoli, B. *Inorg. Chem.* **1999**, *38*, 620−621.
(30) Jullian, V.; Shepherd, E.; Gelbrich, T.; Hursthouse, M. B.; Kilburn, J. D. *Tetrahedron Lett.* **2000**, *41*, 3963−3966.
(31) Prevot-Halter, I.; Smith, T.; Weiss, J. *J. Org. Chem.* **1997**, *62*, 2186−2192.
(32) Prevot-Halter, I.; Weiss, J. *New J. Chem.* **1998**, *22*, 869−874.
(33) Goswami, S.; Ghosh, K. *Tetrahedron Lett.* **1997**, *38*, 4503−4506.
(34) Goswami, S.; Ghosh, K.; Halder, M. *Tetrahedron Lett.* **1999**, *40*, 1735−1738.
(35) Goswami, S.; Ghosh, K.; Dasgupta, S. *J. Org. Chem.* **2000**, *65*, 1907−1914.
(36) Lavigne, J. J.; Anslyn, E. V. *Angew. Chem., Int. Ed.* **1999**, *38*, 3666−3669.
(37) Canary, J. W.; Gibb, B. C. *Prog. Inorg. Chem.* **1997**, *45*, 1−82.
(38) Busch, D. H. *Chem. Rev.* **1993**, *93*, 847−860.
(39) Fabbrizzi, L.; Poggi, A. *Transition metals in supramolecular chemistry*; Kluwer Academic Publishers: Dordrecht and Boston, 1994.
(40) Rybak-Akimova, E. V. *Rev. Inorg. Chem.* **2001**, *21*, 207−298.
(41) Goodman, M. S.; Jubian, V.; Hamilton, A. D. *Tetrahedron Lett.* **1995**, *36*, 2551−2554.
(42) Goodman, M. S.; Hamilton, A. D.; Weiss, J. *J. Am. Chem. Soc.* **1995**, *117*, 8447−8455.
(43) Martell, A. E.; Motekaitis, R. J. *J. Am. Chem. Soc.* **1988**, *110*, 8059−8064.
(44) Motekaitis, R. J.; Martell, A. E. *Inorg. Chem.* **1991**, *30*, 694−700.
(45) Llobet, A.; Reibenspies, J.; Martell, A. E. *Inorg. Chem.* **1994**, *33*, 5946−5951.
(46) Lu, Q.; Reibenspies, J. J.; Martell, A. E.; Motekaitis, R. J. *Inorg. Chem.* **1996**, *35*, 2630−2636.
(47) Lacy, S. M.; Rudkevich, D. M.; Verboom, W.; Reinhoudt, D. N. *J. Chem. Soc., Perkin Trans. 2* **1995**, 135−139.
(48) Cutland, A. D.; Halfen, J. A.; Kampf, J. W.; Pecoraro, V. L. *J. Am. Chem. Soc.* **2001**, *123*, 6211−6212.
(49) Beer, P. D.; Drew, M. G. B.; Hazlewood, C.; Hesek, D.; Hodacova, J.; Stokes, S. E. *J. Chem. Soc., Chem. Commun.* **1993**, 229−231.
(50) Beer, P. D.; Hesek, D.; Kingston, J. E.; Smith, D. K.; Stokes, S. E.; Drew, M. G. B. *Organometallics* **1995**, *14*, 3288−3295.
(51) Jeong, K.-S.; Lee, J. W.; Park, T.-Y.; Chang, S.-Y. *Chem. Commun.* **1999**, 2069−2070.
(52) Tomapatanaget, B.; Tuntulani, T.; Chailapakul, O. *Org. Lett.* **2003**, *5*, 1539−1542.
(53) Busch, D. H.; Alcock, N. W. *Chem. Rev.* **1994**, *94*, 585−623.
(54) Alcock, N. W.; Lin, W. K.; Jircitano, A.; Mokren, J. D.; Corfield, P. W. R.; Johnson, G.; Novotnak, G.; Cairns, C.; Busch, D. H. *Inorg. Chem.* **1987**, *26*, 440−452.
(55) Rybak-Akimova, E. V.; Kuczera, K.; Jas, G. S.; Deng, Y.; Busch, D. H. *Inorg. Chem.* **1999**, *38*, 3423−3434.
(56) Rybak-Akimova, E. V.; Kuczera, K. *Inorg. Chem.* **2000**, *39*, 2462−2472.
(57) Breslow, R.; Yang, J.; Yan, J. M. *Tetrahedron* **2002**, *58*, 653−659.
(58) Belvedere, S.; Breslow, R. *Bioorg. Chem.* **2001**, *29*, 321−331.
(59) Yang, J.; Breslow, R. *Tetrahedron Lett.* **2000**, *41*, 8063−8067.
(60) Yang, J.; Weinberg, R.; Breslow, R. *Chem. Commun.* **2000**, 531−532.
(61) Breslow, R.; Gabriele, B.; Yang, J. *Tetrahedron Lett.* **1998**, *39*, 2887−2890.
(62) Breslow, R.; Dong, S. D. *Chem. Rev.* **1998**, *98*, 1997−2011.
(63) Breslow, R. *Acc. Chem. Res.* **1995**, *28*, 146−153.
(64) French, R. R.; Holzer, P.; Leuenberger, M. G.; Woggon, W.-D. *Angew. Chem., Int. Ed.* **2000**, *39*, 1267−1269.
(65) Woggon, W.-D.; Wagenknecht, H.-A.; Claude, C. *J. Inorg. Biochem.* **2001**, *83*, 289−300.
(66) French, R. R.; Holzer, P.; Leuenberger, M.; Nold, M. C.; Woggon, W.-D. *J. Inorg. Biochem.* **2002**, *88*, 295−304.

receptors and reagents. Metal complexes with Jäger and cyclidene macrocycles display catalytic properties (e.g., cobalt cyclidenes catalyze phenol oxidation;[67] nickel complexes catalyze electroreduction of carbon dioxide into oxalate).[68] Chiral building blocks can be easily incorporated into Jäger and cyclidene platforms,[69,70] opening the possibilities for chiral recognition and enantioselective catalysis.

Earlier we prepared a receptor for dicarboxylic acids based on a 15-membered nickel(II) cyclidene platform with two cyclic tetraamine (cyclen) binding sites, which displayed notable length and shape selectivity.[71] We also observed very similar length selectivity in substrate binding for diammonium recognition by a crown-appended 15-membered Ni(II) cyclidene.[72] We now set out to explore the role of cyclidene molecular shape in the guest binding properties of receptors for dicarboxylates. A series of three nickel(II) complexes bearing two ethylpyridine receptor sites were prepared (**I**−**III**) that were different only in the size of the macrocyclic ring (14-, 15-, and 16-membered, respectively). The inside-the-macrocycle metal binding locked the conformations of the unsaturated chelate rings, thus determining the overall shape of the molecules. Three complexes were crystallographically characterized, and the role of their molecular shape in dicarboxylic acid binding affinities was examined.

Experimental Section

General Methods. Chemicals (reagent grade or better) and anhydrous solvents were purchased from Aldrich or Acros and used as received. Starting dimethoxy cyclidenes [Ni[(MeOEthi)$_2$Me$_2$[14]tetraeneN$_4$]](PF$_6$)$_2$, [Ni[(MeOEthi)$_2$Me$_2$[15]tetraeneN$_4$]](PF$_6$)$_2$, and [Ni[(MeOEthi)$_2$Me$_2$[16]tetraeneN$_4$]](PF$_6$)$_2$ were prepared according to published procedures.[73−76] All measurements were recorded at 298 K, unless otherwise noted. The ^{1}H and ^{13}C NMR spectra were recorded on a Bruker DPX-300 spectrometer and referenced to residual solvent resonance peaks. IR spectra were obtained as KBr pellets on a Mattson RS-1 FTIR spectrometer, UV−vis spectra (190−1100 nm) were recorded in 1-cm quartz cuvettes on a Hitachi U-2000 spectrophotometer. Matrix-assisted laser desoprtion ionization time-of-flight (MALDI-TOF) MS spectra were obtained on a Bruker Biflex MALDI-TOF operating in positive reflectron mode and externally referenced to CsI. Elemental analyses were performed by QTI (Whitehouse, NJ 08888).

Synthesis. [2,9-Dimethyl-3,10-bis[1-[2-(2-pyridineethylamino)ethylidene]-1,5,8,12-tetraazacyclotetradeca-1,4,8,11-tetraene]-nickel(II) Hexafluorophosphate ([Ni[(2-pyEtNHEthi)$_2$Me$_2$[14]tetraeneN$_4$]](PF$_6$)$_2$) (I). [Ni[(MeOEthi)$_2$Me$_2$[14]tetraeneN$_4$]](PF$_6$)$_2$ (0.500 g, 0.734 mmol) was added to 25 mL of dry methanol. To this yellow suspension was added 0.176 mL (1.47 mmol) of 2-aminoethyl(2-pyridine). The color of the liquid phase changed quickly to red upon addition of the amine, but undissolved yellow solid material remained suspended. Acetonitrile (10 mL) was added, and methanol was removed on a rotary evaporator. The concentrated reaction mixture was then treated with an additional amount of acetonitrile (50 mL), yielding a homogeneous solution. A small excess of 2-aminoethyl(2-pyridine) (0.04 mL, 0.33 mmol) was added, and the reaction mixture was stirred at room temperature for 20 min. The reaction mixture was then concentrated on a rotary evaporator, and the orange product precipitated upon addition of methanol. The product was collected by filtration and dried in a vacuum. Yield 0.49 g (77%). Anal. Calcd for NiC$_{30}$H$_{40}$N$_8$P$_2$F$_{12}$: C, 41.83; H, 4.68; N, 13.01. Found: C, 41.84; H, 4.71; N, 12.97. MALDI-TOF-MS (matrix of dithranol) *m*/*z*: 569.1 [(M − H)$^+$], 447.2, 423.1, 301.3, 147.0. ^{1}H NMR (300 MHz, CD$_3$CN, 298 K, δ): 2.20 (s, 6H), 2.39 (s, 6H), 3.17 (t, 4H), 3.44 (s, 8H), 3.97 (t, 4H), 7.26 (m, 2H), 7.32 (d, 2H), 7.70 (s, 2H), 7.75 (m, 2H), 8.52 (m, 2H). ^{13}C NMR (75.5 MHz, CD$_3$CN, δ) (15 signals): 19.3, 22.2, 35.7, 46.0, 56.5, 60.1, 108.9, 123.2, 124.8, 138.3, 150.1, 157.7, 159.3, 166.5, 175.4. IR (KBr) cm^{-1}: 3367 (N−H), 2937, 1624, 1576, 842, 558. UV−vis (CH$_3$CN) λ_{max}, nm (ϵ): 262 sh (24 030), 267 (24 730), 278 sh (22 370), 399 (45 150), 478 (1460).

[2,11-Dimethyl-3,10-bis[1-[2-(2-pyridineethylamino)ethylidene]]-1,5,8,12-tetraazacyclopentadeca-1,4,8,11-tetraene]nickel(II) hexafluorophosphate ([Ni[(2-pyEtNHEthi)$_2$Me$_2$[15]tetraeneN$_4$]](PF$_6$)$_2$) (II) was prepared by a modification of the published procedure.[77] [Ni[(MeOEthi)$_2$Me$_2$[15]tetraeneN$_4$]](PF$_6$)$_2$ (0.200 g, 0.288 mmol) was placed in a 50-mL round-bottom flask and dried for 2 h in an oven. This material was dissolved in 5 mL of dry acetonitrile upon stirring. To this yellow solution, 0.07 mL (0.584 mmol) of 2-aminoethyl(2-pyridine) was added, resulting in an immediate color change to red. The reaction mixture was stirred for 30 min, and the solvent was removed by rotary evaporation. The residue was recrystallized from boiling methanol (20 mL). The red crystals were isolated by filtration. Yield ca. 70%. Anal. Calcd for NiC$_{31}$H$_{42}$N$_8$P$_2$F$_{12}$: C, 42.54; H, 4.84; N, 12.80. Found: C, 42.56; H, 4.89; N, 12.72. MALDI-TOF-MS (matrix of dithranol) *m*/*z*: 729.0 [(M + PF$_6$)$^+$], 582.9 [(M − H)$^+$], 436.9, 315.3, 147.0. ^{1}H NMR (300 MHz, CD$_3$CN, 298 K, δ): 2.11 (s, 6H), 2.34 (s, 6H), 3.17 (t, 4H), 3.25 (s, 4H), 3.66 (t, 4H), 3.97 (t, 4H), 7.26 (m, 2H), 7.32 (m, 2H), 7.63 (s, 2H), 7.74 (m, 2H), 8.49 (m, 2H). ^{13}C NMR (75.5 MHz, CD$_3$CN, δ) (16 Signals): 17.2, 19.9, 26.6, 36.3, 45.4, 47.9, 59.7, 110.5, 123.2, 124.8, 138.2, 150.2, 158.2, 159.3, 167.3, 172.5. IR (KBr) cm^{-1}: 3374 (N−H), 2935, 1624, 1567, 850, 557. UV−vis (CH$_3$CN) λ_{max}, nm (ϵ): 262 sh (17 100), 267 (17 800), 283 (18 670), 379 (45 970), 486 (1080).

[2,12-Dimethyl-3,11-bis[1-[2-(2-pyridineethylamino)ethylidene]-1,5,9,13-tetraazacyclohexadeca-1,4,9,12-tetraene]]nickel(II) Hexafluorophosphate ([Ni[(2-pyEtNHEthi)$_2$Me$_2$[16]tetraeneN$_4$]](PF$_6$)$_2$) (III). [Ni[(MeOEthi)$_2$Me$_2$[16]tetraeneN$_4$]](PF$_6$)$_2$ (0.600 g, 0.846 mmol) was dissolved in 20 mL of dry acetonitrile with stirring, and 0.20 mL (1.67 mmol) of 2-aminoethyl(2-pyridine) was added to the solution. The yellow solution turned red immediately upon addition. After 1 h, the solvent was removed and 20 mL of boiling methanol were added to the residue and left overnight. The next day, the solvent was concentrated to 10 mL and the solution was added to 50 mL of diethyl ether. The orange precipitate was carefully filtered with constant addition of fresh diethyl ether to the funnel during filtration (i.e., the product forms tar from the presence of residual methanol if filtered directly from the methanol−diethyl ether mixture). The powdered orange product was dried under vacuum. Yield 0.586 g (78%). Anal. Calcd for

(67) Deng, Y.; Busch, D. H. *Inorg. Chem.* **1995**, *34*, 6380−6386.
(68) Rudolph, M.; Dautz, S.; Jäger, E. G. *J. Am. Chem. Soc.* **2000**, *122*, 10821−10830.
(69) Du, G.; Ellern, A.; Woo, K. L. *Inorg. Chem.* **2003**, *42*, 873−877.
(70) Cameron, J. H.; Clarke, C. A.; Harvey, H. B.; McCullough, K. J.; Rudolpf, P. A. *J. Chem. Soc., Dalton Trans.* **1996**, 1513−1518.
(71) Kryatova, O. P.; Kolchinski, A. G.; Rybak-Akimova, E. V. *J. Inclusion Phenom. Macrocyclic Chem.* **2002**, *42*, 251−260.
(72) Kryatova, O. P.; Kolchinski, A. G.; Rybak-Akimova, E. V. *Tetrahedron* **2003**, *59*, 231−239.
(73) Cameron, J. H. *J. Chem. Educ.* **1995**, *72*, 1033−1036.
(74) Chen, J.; Ye, N.; Alcock, N. W.; Busch, D. H. *Inorg. Chem.* **1993**, *32*, 904−910.
(75) Riley, D. P.; Busch, D. H. *Inorg. Synth.* **1978**, *18*, 36−44.
(76) Cairns, C. J.; Busch, D. H. *Inorg. Synth.* **1990**, *27*, 261−281.

$NiC_{32}H_{44}N_8P_2F_{12}$: C, 43.21; H, 4.99; N, 12.60. Found: C, 43.32; H, 5.04; N, 12.44. MALDI-TOF-MS (matrix of dithranol) *m*/*z*: 596.9 [$(M - H)^+$], 450.9, 329.3, 147.0. ^{1}H NMR (300 MHz, CD_3CN, 298 K, δ) (broadened spectrum): 1.88 (m, 2H), 2.07 (s, 6H), 2.26 (s, 6H), 3.05 (m, 6H), 3.12 (m, 4H), 3.35 (m, 4H), 3.90−3.63 (m, 4H), 7.22 (m, 2H), 7.28 (m, 2H), 7.51 (s, 2H), 7.70 (m, 2H), 8.47 (m, 2H). ^{13}C NMR (75.5 MHz, CD_3CN, δ) (16 signals): 15.5, 21.0, 30.2, 30.7, 36.7, 45.0, 51.6, 56.4, 112.2, 123.1, 124.8, 138.1, 150.1, 159.5, 160.0, 168.4. IR (KBr) cm^{-1}: 3385 (N−H), 2935, 1614, 1583, 843, 558. UV−vis (CH_3CN) λ_{max}, nm (ϵ): 254 sh (12 610), 260 (12 900), 266 sh (11 360), 336 (37 030), 368 (25 710), 435 sh (570).

NMR Titration Studies. The guest binding to the three molecular tweezers hosts were studied by ^{1}H NMR titrations[78−80] of the macrocyclic complexes with dicarboxylic acid guests. A 5 mM solution of a host (**I**−**III**) was prepared in CD_3CN, and 0.500 mL was added to a 5 mm NMR tube. After the ^{1}H NMR spectrum was recorded, aliquots of a prepared solution of a dicarboxylic acid in CD_3CN were added and spectra were recorded. In some cases, solubility of the dicarboxylic acid was limiting; therefore the concentration could not be determined gravimetrically. Therefore in all cases the concentration was determined by integration of the appropriate signals of the host and the guest. The 1:1 stoichiometry of guest binding was determined by Job's plots.[78−82] Experimental titration curves were fit by nonlinear regression to a 1:1 binding model (eq 1)[80] using a spreadsheet program, yielding the values of the association constants

$$\delta_{calc} = \delta_h + \frac{(\delta_c - \delta_h)}{2}\left\{\left(\frac{[G]_t}{[H]_t} + \frac{1}{K_a[H]_t} + 1\right) \pm \left[\left(\frac{[G]_t}{[H]_t} + \frac{1}{K_a[H]_t} + 1\right)^2 - 4\frac{[G]_t}{[H]_t}\right]^{1/2}\right\} \quad (1)$$

where δ_{calc} is the calculated chemical shift, δ_h, δ_c, and K_a are optimized in the least-squares routine and represent the chemical shift of the host signal in the absence of binding, the signal arising from complexation, and the binding constant, respectively, and $[G]_t$ and $[H]_t$ are the total concentrations (dilution effects included) in the NMR tube of the respective species.

Nuclear Overhauser Effect Spectrometry (NOESY) Experiments. A degassed sealed NMR tube containing a 20 mM solution of 1:1 **II**−maleic acid in CD_3CN was prepared by freeze−pump−thaw methods. The 300 MHz-2D NOESY spectrum was obtained with a 500 ms mixing time.

X-ray Crystallography. [Ni[(2-pyEtNHEthi)$_2$Me$_2$[14]tetraeneN$_4$]](PF$_6$)$_2$ (I). Orange needles of **I** were grown from ether diffusion into a 1:2 acetonitrile−methanol mixture. All measurements were made on a Rigaku RAXIS imaging plate area detector with graphite monochromated Mo Kα radiation. A suitable single crystal of **I** was mounted on a glass fiber. The data were collected at room temperature to a maximum 2θ value of 60.1°. Of the 24 611 reflections that were collected, 11 096 were unique ($R_{int} = 0.291$); equivalent reflections were merged. The linear absorption coefficient μ, 7.26 cm^{-1} for Mo Kα radiation, was applied, which resulted in transmissions factors ranging from 0.195 to 0.944. The data were corrected for Lorentz and polarization effects. A correction for secondary extinction[83] was applied (coefficient = 938.33). The observed systematic absences uniquely determined the space group to be *Pbca* (No. 61). The structure was solved by direct methods[84] and expanded using Fourier techniques.[85] The non-hydrogen atoms were refined anisotropically. Hydrogen atoms were refined isotropically. The final cycle of full-matrix least-squares refinement[86] on F was based on 1296 observed reflections ($I > 3.00\sigma(I)$) and 262 variable parameters and converged (largest parameter shift was 0.031 times its esd) with unweighted and weighted agreement factors of $R = \sum||F_o| - |F_c||/\sum|F_o| = 0.074$ and $R_w = [\sum w(|F_o| - |F_c|)^2/wF_o^2]^{1/2} = 0.076$.

The standard deviation of an observation of unit weight[86] was 1.193. The weighting scheme was based on computing.[87] Plots of $\sum w(|F_o| - |F_c|)^2$ vs $|F_o|$, reflection order in data collection, $\sin\theta/\lambda$, and various classes of indices showed no unusual trends. The maximum and minimum peaks on the final difference Fourier map corresponded to 0.68 and −0.50 e$^-$/Å^3, respectively.

Neutral atom scattering factors were taken from Cromer and Waber.[88] Anomalous dispersion effects were included in F_{calc};[89] the values for $\Delta f'$ and $\Delta f''$ were those of Creagh and McAuley.[90] The values for the mass attenuation coefficients are those of Creagh and Hubbell.[91] All calculations were performed using the CrystalStructure[92,93] crystallographic software package.

The structure of 14NHEt$_2$Py (**I**) is centrosymmetric with $^1/_2$ molecule per asymmetric unit with the Ni atom lying on an inversion center. Details of the data collection and refinement are given in Table 1.

[Ni[(2-pyEtNHEthi)$_2$Me$_2$[15]tetraeneN$_4$]](PF$_6$)$_2$ (II) and [Ni[(2-pyEtNHEthi)$_2$Me$_2$[16]tetraeneN$_4$]](PF$_6$)$_2$ (III). Red needles of **II** were obtained from ether diffusion in a 1:2 acetonitrile−methanol mixture, and red-yellow blocks of **III** were obtained upon evaporation of a 1:1 acetonitrile−methanol solution. Data were collected using a Bruker SMART CCD-based diffractometer equipped with an LT-3 low-temperature apparatus operating at 213 K. Suitable crystals were chosen and mounted on a glass fiber using paratone oil. Data were measured using omega scans of 0.3° per frame (for

(77) Schammel, W. P.; Zimmer, L. L.; Busch, D. H. *Inorg. Chem.* **1980**, *19*, 3159−3167.
(78) Sahai, R.; Loper, G. L.; Lin, S. H.; Eyring, H. *Proc. Natl. Acad. Sci. U. S. A.* **1974**, *71*, 1499−1503.
(79) Fielding, L. *Tetrahedron* **2000**, *56*, 6151−6170.
(80) Hirose, K. *J. Inclusion Phenom. Macrocyclic Chem.* **2001**, *39*, 193−209.
(81) Gil, V. M. S.; Oliveira, N. C. *J. Chem. Educ.* **1990**, *67*, 473−478.
(82) Nowick, J. S.; Chen, J. S.; Noronha, G. *J. Am. Chem. Soc.* **1993**, *115*, 7636−7644.
(83) Larson, A. C. In *Crystallographic Computing*, Proceedings of an International Summer School organized by The Commission on Crystallographic Computing of the International Union of Crystallography, Ottawa, Ontario, Canada, 1969; Ahmed, F. R., Hall, S. R., Huber, C. P., Eds.; Munksgaard: Copenhagen, 1970; pp 291−294. (Equation 22, with V replaced by the cell volume.)
(84) *SIR92*: Altomare, A.; Cascarano, G.; Giacovazzo, C.; Guagliardi, A.; Burla, M.; Polidori, G.; M., C. *J. Appl. Crystallogr.* **1994**, *27*, 435.
(85) Beurskens, P. T.; Admiraal, G.; Beurskens, G.; Bosman, W. P.; de Gelder, R.; Israel, R.; Smits, J. M. M. DIRDIF99 *The DIRDIF-99 program system, Technical Report of the Crystallography Laboratory*; University of Nijmegen: The Netherlands, 1999.
(86) Least-squares function minimized: $\sum w(|F_o| - |F_c|)^2$ where w = least-squares weights.
(87) Carruthers, J. R.; Watikin, D. J. *Acta Crystallogr.* **1979**, *A35*, 698−699.
(88) Cromer, D. T.; Waber, J. T. *International Tables for X-ray Crystallography*; The Kynoch Press: Birmingham, England, 1974; Vol. IV, Table 2.2A.
(89) Ibers, H. A.; Hamilton, W. C. *Acta Crystallogr.* **1964**, *17*, 781.
(90) Creagh, D. C.; Mcauley, W. J. *International Tables for Crystallography*; Wilson, A. L. C., Ed.; Kluwer Academic Publishers: Boston, 1992; Vol. C, pp 219−222, Table 4.2.6.8.
(91) Creagh, D. C.; Hubbell, J. H. *International Tables for Crystallography*; Wilson, A. L. C., Ed.; Kluwer Academic Publishers: Boston, 1992; Vol. C, pp 200−206, Table 4.2.4.3.
(92) CrystalStructure 2.00 *Crystal Strucutre Analysis Package*; Ricgaku and MSC: 2001.
(93) Watikin, D. J.; Prout, C. K.; Carruthers, J. R.; Betteridge, P. W. CRYSTALS Issue 10 Chemical Crystallography Laboratory: Oxford, U.K.,

Table 1. Crystal Data and Structure Refinement Parameters

	[14]NHEt2Py, **I**[a]	[15]NHEt2Py, **II**[b]	[16]NHEt2Py, **III**[b]
formula	$NiC_{30}N_8H_{40}P_2F_{12}$	$NiC_{31}N_8H_{42}P_2F_{12}$	$NiC_{32}N_8H_{44}P_2F_{12}$
fw	861.33	875.38	889.40
diffractometer type	Rigaku RAXIS−RAPID	Bruker SMART-CCD	Bruker SMART-CCD
T (K)	296.2	213.2	213.2
λ(Mo Kα) (Å)	0.7107	0.71073	0.71073
cryst size (mm^3)	0.30 × 0.08 × 0.10	0.10 × 0.06 × 0.06	0.14 × 0.20 × 0.20
cryst color (habitat)	orange (needle)	red (needle)	red-yellow (chunk)
cryst syst	orthorhombic	triclinic	triclinic
space group	*Pbca* (No. 61)	$P\bar{1}$ (No. 2)	$P\bar{1}$ (No. 2)
a (Å)	15.484(5)	10.395(3)	10.410(2)
b (Å)	10.661(2)	12.555(4)	17.410(4)
c (Å)	21.810(8)	14.449(5)	21.691(5)
α (deg)	89.73(2)	90.420(6)	101.281(4)
β (deg)	89.97(2)	98.703(6)	94.274(5)
γ (deg)	90.18(2)	97.208(6)	90.852(5)
V (Å^3)	3600.2(2)	1848.5(10)	3842.8(15)
Z	4	2	4
μ_{calcd} (mm^{-1})	0.726	0.708	0.683
d_{calcd} (g cm^{-3})	1.589	1.573	1.537
F_{000}	1768	900	1832
limiting indices	$-19 \le h \le 20$, $-13 \le k \le 13$, $-30 \le l \le 30$	$-12 \le h \le 12$, $-10 \le k \le 14$, $-17 \le l \le 16$	$-11 \le h \le 13$, $-23 \le k \le 17$, $-28 \le l \le 28$
reflns collected	24611	9982	28503
unique reflns	4932 (R_{int} = 0.291)	6462 (R_{int} = 0.0539)	18871 (R_{int} = 0.0456)
reflns with [$F_o^2 > 2\sigma(F_o^2)$]	1296	5100	12894
no. of parameters	262	487	991
ref/para ratio	4.9	13.3	13.01
GOF (S)	1.193	1.141	1.093
R1/wR2 $I > 2\sigma I$	0.0740/−	0.0897/ 0.1977	0.0801/ 0.2434
R1/wR2 all data	−/0.0760	0.1125/ 0.2099	0.1039/ 0.2636
final diff ρ max (e/Å^3)	+0.68−0.50	+0.765−0.441	+1.428−1.337

[a] Structure **I**: refinement using reflections with $F^2 > 3\sigma(F^2)$. The weighted R factor (wR), goodness of fit (S), and R factor (gt) are based on F, with F set to zero for negative F. The threshold expression of $F^2 > 2\sigma(F^2)$ is used only for calculating R factor (gt). [b] Structures **II** and **III**: refinement of F^2 against all reflections. The weighted R factor (wR) and goodness of fit (S) are based on F^2, conventional R factors R are based on F, with F set to zero for negative F^2. The threshold expression of $F^2 > 2\sigma(F^2)$ is used only for calculating R factors (gt) etc. and is not relevant to the choice of reflections for refinement. R factors based on F^2 are statistically about twice as large as those based on F, and R factors based on all data will be even larger.

5 s for **II** and for 30 s for **III**), such that a hemisphere was collected. A total of 1271 frames were collected with a maximum resolution of 0.80 Å for **II** and 0.75 Å for **III**. The first 50 frames were recollected at the end of data collection to monitor for decay. The crystals used for the diffraction study showed no decomposition during data collection. Cell parameters were retrieved using SMART[94] software and refined using SAINT on all observed reflections. Data reduction was performed using the SAINT[95] software, which corrects for Lorentz polarization and decay. The structures were solved by the direct method using the SHELXS-97[96] program and refined by least-squares method on F^2, SHELXL-97,[97] incorporated in SHELXTL V5.10.[98] The space group $P\bar{1}$ (No. 2) was determined for **II** and **III** by analysis of systematic absences. All non-hydrogen atoms were refined anisotropically. Hydrogens were calculated by geometrical methods and refined as a riding model. Details of the data collection and refinement are given in Table 1.

Results

Synthesis and Characterization. The synthesis of molecular tweezers **I**−**III** (Scheme 1) is based on a general reaction of the O-alkylated Jäger macrocycles with amines developed by Busch and co-workers.[53] The scope of this reaction is somewhat limited: while aliphatic primary amines and sterically nonhindered aliphatic secondary amines react smoothly with Jäger macrocycles;[77,99,100] in many cases, steric hindrance prevents or retards cyclidene formation.[77,101] The aromatic amino group is far less reactive and can hardly be attached to Jäger platforms.[77,102] An additional complication is caused by the relative instability of cyclidenes in the presence of strong bases (such as secondary amines) that promote deacylation of Jäger and cyclidene macrocycles.[102,103] These limitations influenced our choice of the receptor groups for carboxylates to be attached to a cyclidene platform. The relatively weak base pyridine was attached via a sterically nonhindered primary amino group in the aminoethyl sidearm. The preparation of complex **II** (the 15-membered platform) has been briefly described by Busch and co-workers.[77] As expected, attaching aminoethylpyridine groups to the 14- and 16-membered platforms also proceeded in high yield, giving rise to target complexes **I** and **III**. All

(94) SMART V 5.054 (NT) *Software for the CCD Detector System*; Bruker Analytical X-ray Systems: Madison, WI, 1998.
(95) Saint V 6.02 (NT) *Software for the CCD Detector System*; Bruker Analytical X-ray Systems: Madison, WI, 2000.
(96) Sheldrick, G. M. SHELXS-90 *Program for the Solution of Crystal Structure*; University of Göttingen: Germany, 1990.
(97) Sheldrick, G. M. SHELXL-97 *Program for the Refinement of Crystal Structure*; University of Göttingen: Germany, 1997.
(98) SHELXTL 6.10 (PC/NT-Version) *Program library for Structure Solution and Molecular Graphics*; Bruker Analytical X-ray Systems: Madison, WI, 2000.
(99) Meade, T. J.; Alcock, N. W.; Busch, D. H. *Inorg. Chem.* **1990**, *29*, 3766−3776.
(100) Takeuchi, K. J.; Busch, D. H.; Alcock, N. W. *J. Am. Chem. Soc.* **1983**, *105*, 4261−4270.
(101) Cameron, J. H.; Scott, E. L. *J. Chem. Soc., Dalton Trans.* **1995**, 1029−1034.
(102) Horwitz, C. P.; Navarro, R.; Dailey, G. C. *Inorg. Chem.* **1990**, *29*, 4262−4268.
(103) Nazarenko, A. Y.; Robinson, P. D.; Wilson, R. M.; Kolchinski, A. G.; Disch, J. S.; Rybak-Akimova, E. V. *J. Inclusion Phenom. Macrocyclic Chem.* **2002**, *42*, 83−87.

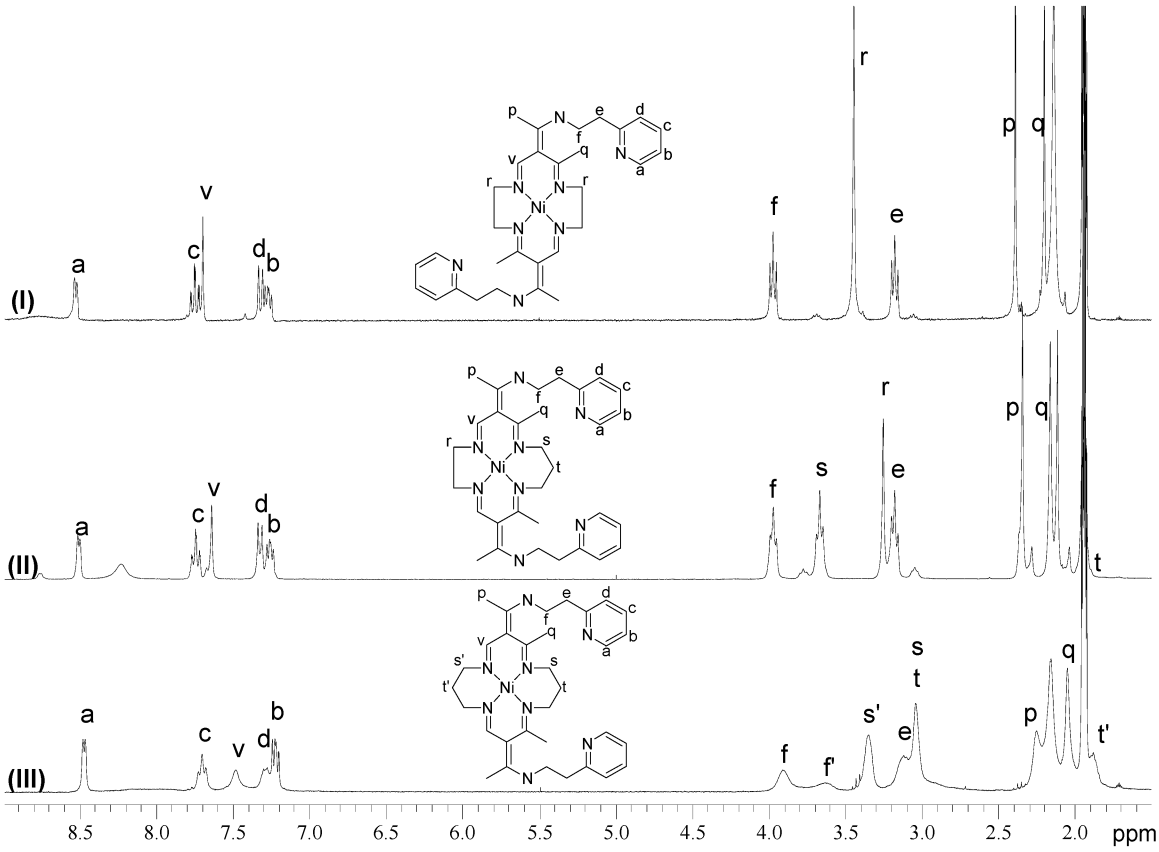

Figure 1. ^{1}H NMR of **I**−**III** in CD_3CN at 298 K. Letters denote proton assignments according to inserts.

three low-spin nickel(II) complexes **I**−**III** were fully characterized (see Experimental Section and Supporting Information (SI) for the analytical and spectroscopic data, including assignments of the NMR spectra). The complexes were stable in the solid state and in both protic and aprotic solvents. Additionally, the absence of a characteristic doublet at 4.8 ppm in the proton NMR spectra, indicative of a bridgehead proton in the deacylated product,[103] confirms that no loss of acyl substituents from the cyclidene platforms has occurred. The aminoethylpyridine-substituted cyclidenes are more stable toward self-decomposition than cyclene-appended cyclidenes that undergo rapid self-decomposition in protic solvents.[71]

The proton NMR spectra of **I**−**III** were similar to each other in their chemical shifts, although the spectrum of **III** showed substantial line broadening (Figure 1). Variable-temperature ^{1}H NMR was conducted on **I** and **III** to elucidate the signal assignment and the origin of line broadening (in particular, to distinguish between an effect of possible paramagnetic impurities in the sample vs a dynamic behavior of the complexes). Upon the heating of sample **I** in CD_3CN, all signals in the ^{1}H NMR become broadened. In contrast, when compound **III** in CD_3CN was heated, all of the signals sharpened, allowing for signal assignment (Figure 2). The most dramatic change was seen in the signals labeled f and f′ that were assigned to methylene protons adjacent to the amine in the receptor arms. At room temperature they exist as two broad peaks with an integration of 3:1, but upon heating to 338 K they coalesce into a well-defined triplet with a chemical shift of the weighted average of the broad signals. Very similar temperature-dependent NMR spectra observed by Cameron and co-workers for the benzyl-appended 16-membered cyclidene were attributed to a conformational equilibrium between the structures with one substituent "capping" the cavity.[104,105] A relatively slow exchange at room temperature reveals different environments for the protons adjacent to the exocyclic nitrogens, whereas at faster equilibrium they give the expected averaged NMR signal. The other signal of the aliphatic protons on the ethylpyridine receptor arms (signal e) resolves into a triplet and shifts slightly to higher field upon heating (correlation spectroscopy (COSY) revealed that e and f are coupled, see SI).

The UV−vis spectra of compounds **I**−**III** in acetonitrile reveal the usual features for square-planar nickel(II) cyclidene complexes:[73,106] the broad absorption bands with λ_{max} at 430−480 nm due to d−d transitions and the charge-transfer bands between 330 and 410 nm (Figure 3.) As the macrocycle ring size increases from 14- to 16-membered, the d−d transition is blue shifted. This can be explained by the fact that increasing the tetraaza macrocycle size increases the metal−

(104) Cameron, J. H.; Scott, E. L. *J. Chem. Soc., Dalton Trans.* **1993**, 3821−3822.
(105) Cameron, J. H.; Clarke, C. A.; Rosair, G.; Scott, E. L. *Coord. Chem. Rev.* **1998**, *174*, 313−326.
(106) Streeky, J. A.; Pillsbury, D. G.; Busch, D. H. *Inorg. Chem.* **1980**, *19*, 3148−3159.

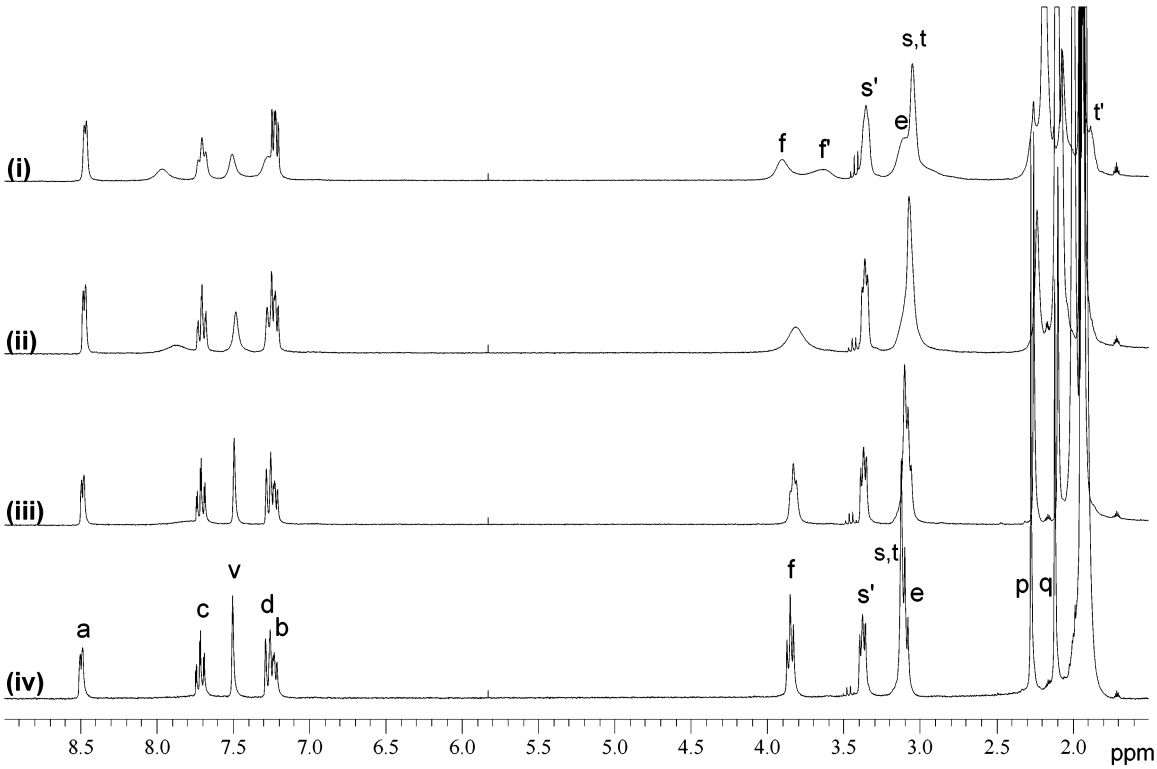

Figure 2. Variable-temperature ^{1}H NMR of **III** in CD_3CN at 293 K (i), 308 K (ii), 323 K (iii), and 338 K (iv). See Figure 1 for atom labeling scheme.

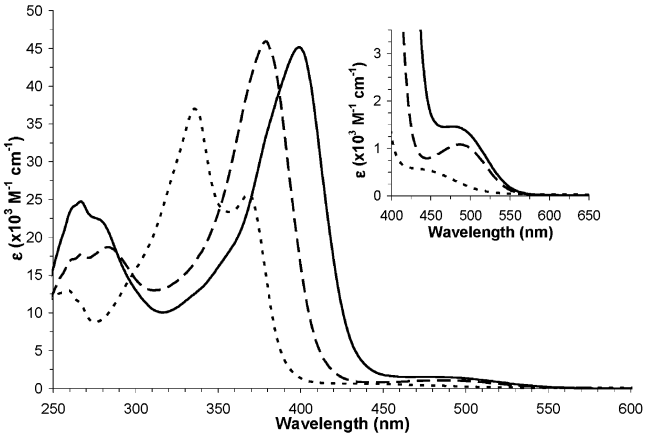

Figure 3. UV−vis spectrum of **I**−**III** in acetonitrile at room temperature: **I** (solid), **II** (dashed), **III** (dotted).

nitrogen distances, which, in turn, increases the HOMO−LUMO gap.[73] The d−d transition in **II,** however, is very similar in energy to that in **I**, possibly due to distortion of the 15-membered macrocycle. A systematic blue shift in the series **I**, **II**, and **III** is seen for the charge-transfer bands. Very similar trends in UV−vis spectra have been reported previously for Jäger and cyclidene complexes with variable ring size.[73,106] The absorption bands in UV−vis spectrum of **III** (λ_{max} (ϵ) 336 (37 030), 368 (25 710), 435 sh nm (570), see Experimental Section) are almost identical to the spectrum of the analogous benzyl-substituted cyclidene prepared by Cameron and co-workers (λ_{max} (ϵ) 333 (39 800), 363 (19 950), and 443 nm (10 00)),[101] thus confirming a similar electronic structure of these two compounds and indicating the lack of pyridine coordination in **III**.

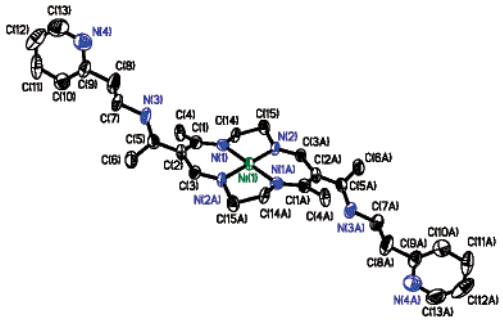

Figure 4. ORTEP diagram of [Ni(2-pyEtNH[14]cyclidene)]$(PF_6)_2$ complex **I**. Hydrogens and counteranions are omitted for clarity. Thermal ellipsoids are shown at 50% probability.

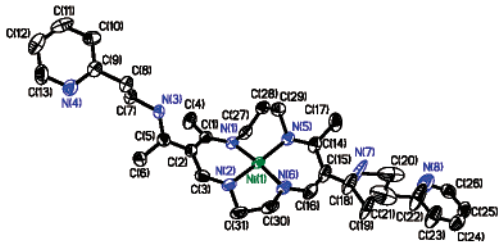

Figure 5. ORTEP diagram of [Ni(2-pyEtNH[15]cyclidene)]$(PF_6)_2$ complex **II**. Hydrogens and counteranions are omitted for clarity. Thermal ellipsoids are shown at 50% probability.

X-ray Structures of the Macrocyclic Hosts. The crystal structures of three nickel(II) complexes **I**−**III** are shown in Figures 4−6 (the PF_6^- anions are omitted for clarity). The structure of the 14-membered macrocycle **I** is centrosymmetric, with the Ni atom lying on an inversion center. The symmetry is lost in the 15- and 16-membered macrocyclic complexes. Two independent complex cations are present in the asymmetric unit of the 16-membered complex (one

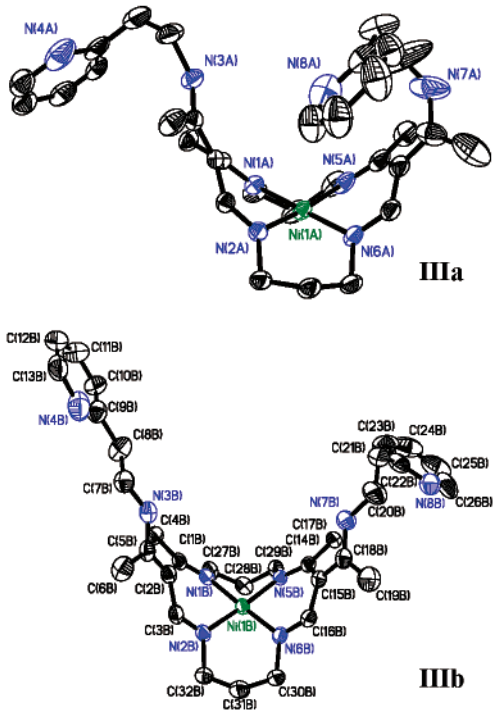

Figure 6. ORTEP diagram of [Ni(2-pyEtNH[16]cyclidene)]$(PF_6)_2$ complex **IIIa** (top) and **IIIb** (bottom). Hydrogens and counteranions are omitted for clarity. Thermal ellipsoids are shown at 50% probability.

in a capped configuration labeled **IIIa** and one in an open configuration labeled **IIIb** in Figure 6). Crystal packing (see SI) indicates that in all structures, N3 and N7 (the nitrogen atoms from the bridgehead NH groups) are within hydrogen bonding distance to PF_6^- anions and the arene ring of a pyridine pendant arm is π-stacking with the extended conjugated NiN1C1C2C3N2 ring system of the unsaturated chelate rings in the macrocycles.

The analysis of the structural features of cations **I**−**III** reveals the systematic variations in the structures of the unbridged cyclidenes that are different only in their macrocyclic ring size. The monocyclic compounds **I**−**III** follow the general trends established by Busch, Alcock, and co-workers on a large series of lacunar (bicyclic or bridged) cyclidenes and their precursors.[53,54,107]

In the immediate nickel(II) coordination sphere, the Ni−N bond lengths are typical for low-spin nickel(II) complexes.[108] The average Ni−N bond distances increase in the series **I** (1.841 Å) < **II** (1.865 Å) < **IIIb** (1.883 Å) ≈ **IIIa** (1.886 Å) (Table 2). This trend can be attributed to the larger macrocyclic size in the latter compounds. The larger saturated six-membered chelate rings allow for an increase in the bite angle in the series (i.e., the N1−Ni−N5 and N2−Ni−N6 bond angles in the saturated chelate rings increase in the series **I** < **II** < **III**; simultaneously, the bond angles N1−Ni−N2 and N5−Ni−N6, in the unsaturated six-membered chelate rings, decrease with an increase in the macrocyclic ring size).

The NiN_4 plane in **I** is flat with no deviation from planarity due to the inversion center on the nickel atom. Structures **II**, **IIIa**, and **IIIb** show only slight variations in the planarity of the nickel coordination sphere, with the larger mean deviation of Ni(II) from the N_4 plane (0.1085 Å) found for structure **II.** This distortion from the planar NiN_4 geometry in the 15-membered **II** can be attributed to the skew conformation of the five-membered chelate ring on one side of the macrocycle.

The most dramatic effect of the macrocyclic ring size in cyclidene complexes can be seen in the overall shape of the molecules (Figures 4−6). Busch and Alcock established that, in general, the 14-membered cyclidenes are essentially flat in nature, whereas 16-membered cyclidenes fold and usually adopt a saddle-shaped configuration.[53] An "open", Z-shaped configuration was also reported for a trans-substituted 16-membered Jäger macrocycle.[109] Because of the presence of both a five- and a six-membered saturated chelate ring, the 15-membered cyclidenes are known to exist in either planar or saddle-shaped configurations.[53]

The (2-pyridyl)ethylamino-appended cyclidenes **I**−**III** follow these general trends. The size and conformation of saturated chelate rings clearly induce the orientation of the unsaturated "wings" of the cyclidene platform. In compound **I**, the two five-membered saturated chelate rings are sterically constrained in a skew conformation. They buckle in opposite directions, which stabilizes the planar nature of structure **I**. Compound **II** also crystallized in an extended configuration; however, here five- and six-membered saturated chelate rings (both in a skew conformation) are buckled in the same direction. This results in the zigzag, Z shape observed where the NiN1C1C2C3N2 unsaturated chelate rings are nearly coplanar (but tilted with respect to the NiN_4 plane). This is drastically opposed to the structures of **IIIa** and **IIIb** in which the larger six-membered saturated rings have adopted a boat and a chair conformation. This is the typical orientation of the saturated metallo chelate rings in 16-membered cyclidenes, and subsequently this leads to the saddle shape of the platform.[54]

To quantitatively describe the shape of the cyclidenes, Busch and co-workers have devised a series of angular parameters, namely, saddle angles α, β, and γ and torsional angles δ and ϵ (See Chart 1, Table 3 for definitions.) Saddle angles α and β define the shape of cleftlike molecules, but they are equal or close to 0° in molecules **I** and **II**, respectively, as the unsaturated chelate rings in them are essentially coplanar. However observation of "local" angles, the angle between adjacent N1N2C1C3 and C1C2C3 planes (γ) and the angle between adjacent N1N2N1′N2′ and N1N2C1C3 (which we define as ζ), are more indicative of the unsaturated "wings" bowed nature in centrosymmetric, flat, or Z-shaped cyclidenes. As the macrocycle is increased in size, an increase in the torsional angles between the three planes defining a "wing" is clearly seen (Table 3). The saddle shape of the cyclidene platform in **IIIa** and **IIIb** is obvious,

(107) Alcock, N. W.; Padolik, P. A.; Pike, G. A.; Kojima, M.; Cairns, C. J.; Busch, D. H. *Inorg. Chem.* **1990**, *29*, 2599−2607.
(108) Sacconi, L.; Mani, F.; Bencini, A. *Comprehensive Coordination Chemistry*; Wilkinson, G., Gillard, R. D., McCleverty, J. A., Eds.; Pergamon Press: New York, 1987; Vol. 5, p 86.
(109) Cameron, J. H.; Nicol, D. P.; Rosair, G. M. *Chem. Commun.* **1998**, 1595−1596.

Table 2. Selected Bond Lengths (Å) and Angles (deg) for Compounds **I**−**III**[a]

	[14]NHEt2Py	[15]NHEt2Py	[16]NHEt2Py-capped	[16]NHEt2Py-open
Ni(1)−N(1)	1.867(7)	1.884(5)	1.890(3)	1.883(3)
Ni(1)−N(2)	1.814(6)	1.846(5)	1.879(3)	1.874(3)
Ni(1)−N(5)		1.880(5)	1.889(3)	1.896(3)
Ni(1)−N(6)		1.847(5)	1.886(3)	1.877(3)
N(1)−C(1)	1.31(1)	1.304(7)	1.299(4)	1.303(5)
C(1)−C(2)	1.444(12)	1.443(8)	1.461(5)	1.466(5)
C(2)−C(3)	1.429(11)	1.424(8)	1.434(5)	1.438(6)
N(2)−C(3)	1.282(9)	1.290(8)	1.289(4)	1.279(5)
C(1)−C(4)	1.511(11)	1.494(8)	1.501(5)	1.512(5)
C(2)−C(5)	1.400(11)	1.434(8)	1.399(5)	1.403(6)
C(5)−C(6)	1.516(13)	1.479(9)	1.502(6)	1.511(6)
N(3)−C(5)	1.303(11)	1.310(7)	1.331(5)	1.320(6)
N(5)−C(14)		1.308(8)	1.301(6)	1.297(5)
C(14)−C(15)		1.470(9)	1.444(7)	1.467(5)
C(15)−C(16)		1.428(9)	1.419(6)	1.430(5)
N(6)−C(16)		1.289(8)	1.294(5)	1.292(5)
C(14)−C(17)		1.509(10)	1.527(6)	1.501(5)
C(15)−C(18)		1.413(9)	1.416(7)	1.411(5)
C(18)−C(19)		1.499(10)	1.536(9)	1.519(6)
N(7)−C(18)		1.316(10)	1.329(7)	1.312(6)
N(1)−Ni(1)-N(2)	93.1(7)	91.2(2)	88.13(13)	88.07(13)
N(1)−Ni(1)-N(5)	86.8(3)	92.4(2)	91.37(14)	91.08(13)
N(5)−Ni(1)-N(6)		91.6(2)	88.77(14)	88.77(13)
N(2)−Ni(1)-N(6)		86.0(2)	91.55(13)	91.81(13)
N(1)−Ni(1)-N(6)	180	171.4(2)	178.70(14)	176.83(14)
N(2)−Ni(1)-N(5)		170.8(2)	172.31(15)	175.00(15)
C(1)−C(2)-C(3)	119.6(7)	120.8(5)	115.7(3)	116.4(4)
C(1)−C(2)-C(5)	121.0(7)	122.4(5)	123.5(3)	122.3(4)
C(2)−C(5)-C(6)	121.1(8)	122.7(5)	122.9(4)	121.1(4)
C(14)−C(15)-C(16)		119.9(6)	117.7(4)	117.0(3)
C(14)−C(15)-C(18)		122.5(7)	124.8(4)	122.4(4)
C(15)−C(18)-C(19)		122.5(7)	122.0(5)	122.3(4)

[a] Atom numbering for **I**−**III** corresponds to ORTEP plots (Figures 4−6).

Chart 1. Parameters Used To Define Saddle Shape[a] [54]

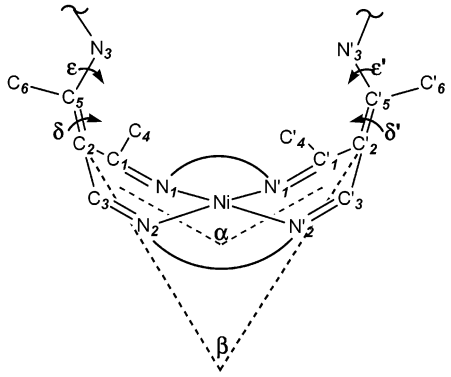

[a] Key: α, the angle between equivalent (N1N2C1C3) planes; β, the angle between two equivalent (C1C2C3) planes; γ, the angle between adjacent (N1N2C1C3) and (C1C2C3) planes (=0.5(α − β)); ζ, the angle between adjacent (N1N2N1′N2′) and (N1N2C1C3) planes; δ, dihedral angle of bond C2−C5; and ϵ, dihedral angle of bond C5−N3.

while the curvature of **I** and **II** is masked by the opposite directions of the "wing" tilting relative to the NiN_4 plane. If the bowing effect of S-shaped (flat and Z-shaped cyclidenes) was additive rather than subtractive, this would amount to a U-shaped saddle angle for structures **I** (α = 162°, β = 137°) and **II** (α = 131°, β = 98°). In the case of **IIIa** and **IIIb**, saddle angles α and β are properly defined and as such are (97.8° and 47.5°) for **IIIa** and (96.9° and 48.3°) for **IIIb**. When torsional angles between the capped variant **IIIa** and the open variant **IIIb** are compared, the small differences in angles (−1.0° for α and +0.8° for β) impart some variation to the cavity size (the distance of C2−C2′ shortens 0.012 Å whereas C5−C5′ lengthens by 0.045 Å).

Torsional angels δ and ϵ depict both the degree of conjugation of N3H into the macrocycle and the orientation of the ethylpyridine arm. Because of strain, the torsional angle δ is typically in the region of 5−20° and ϵ deviates only slightly from 180°.[105] The torsional angle δ in **I**−**III** materials is in the range of 20.3−32.2°, which is typical for cyclidenes.[105] Interestingly, ϵ, which is 172.4° in structure **IIIb**, becomes 37.1° in structure **IIIa**. This large twist places the ethyl pyridine arm into the cavity of the cyclidene. A similar "capping" orientation of the benzyl substituent attached to a [16]cyclidene platform was reported by Cameron.[105] In both structures (**IIIa** and benzyl-cyclidene), the "capping" group is attached to the bridgehead nitrogen atom in a "lid-off" orientation (where the substituent points down, toward the cyclidene platform.)[110] Another example of a capping orientation of an aromatic substituent (a pyrazolyl group) reported by Busch and co-workers[54] did not require a lid-off orientation of the substituent. All other receptor arms (ethylpyridine groups) in **I**−**III** are in the "lid-on" orientation. The substantial flexibility of the receptor arms is reflected in several different orientations of these substituents observed in a single crystal of **III** (two independent molecules in the asymmetric unit are different primarily in the conformations of the ethylpyridine groups).

(110) Busch, D. H.; Jackels, S. C.; Callahan, R. C.; Grzybowski, J. J.; Zimmer, L. L.; Kojima, M.; Olszanski, D. J.; Schammel, W. P.; Stevens, J. C.; Holter, K. A.; Mocak, J. *Inorg. Chem.* **1981**, *20*, 2834−2844.

Table 3. Parameters Used To Define Saddle-Shape of Cyclidenes[a]

saddle parameters	[14]NHEt2Py, **I**	[15]NHEt2Py, **II**	[16]NHEt2Py-capped, **IIIa**	[16]NHEt2Py-open, **IIIb**
dev Ni from NiN_4	0.00	0.0051	−0.0734	−0.0535
dev N1 from NiN_4	0.00	0.1280	−0.0528	−0.0014
dev N2 from NiN_4	0.00	−0.1410	0.0529	0.0281
dev N5 from NiN_4	0.00	−0.1303	0.0524	0.0278
dev N6 from NiN_4	0.00	0.1382	−0.0525	−0.0011
mean dev of NiN_4 plane	0.00	0.1085	0.0526	0.0224
C2−C2′, Å	6.490	6.384	5.258	5.246
C5−C5′, Å	9.223	9.110	6.661	6.706
N3−N3′, Å	10.659	10.267	6.707	6.785
α, deg			97.8	96.8
β, deg			47.5	48.3
γ, γ', deg	12.5, 12.5	14.9, 18.1	28.3,22.1	25.2, 23.4
ζ, ζ', deg	171.2, −171.2	154.9, −156.1	137.9, 139.9	137.2, 139.6
δ, δ', deg	29.7, −	32.3, 26.9	20.4 31.4	24.0, 26.0
ϵ, ϵ', deg	174.5, −	170.4, 155.2	177.7, 37.1	171.8, 172.5

[a] Saddle parameters are defined according to Chart 1.

Table 4. Equilibrium Constants (K_a, M^{-1}) for Carboxylic Acid Binding to Macrocyclic Hosts **I**−**III** at 298 K[a]

guest	pK_a[b]	[14]NHEt2Py, **I**	[15]NHEt2Py, **II**	[16]NHEt2Py **III**
phthalic	2.95; 5.41	19 ± 2	121 ± 12	252 ± 3
3-nitrophthalic	2.11; 4.48	20 ± 2[f]	45 ± 7	421 ± 15
5-nitroisophthalic	3.93; 5.16[d]	64 ± 6	152 ± 7	51 ± 19
2-nitroterephthalic	1.75; 3.60[c]		<10	<10
maleic	1.92; 6.22	100 ± 14	159 ± 13[e]	213 ± 19
benzoic	4.21		0[g]	
fumaric	3.03; 4.38[c]		<10	
2-nitrobenzoic	2.1		<10	<10
4-nitrobenzoic	3.45		<10	<10
nitrobenzene			0[g]	
terephthalic	3.54; 4.34	(insoluble)		
isophthalic	3.5; 4.5 (H_2O)4.78; 5.98[d]	(insoluble)		
trifluoroacetic		2:1 at saturation	2:1 at saturation	

[a] Unless otherwise noted, the NMR titrations were performed in CD_3CN at 298 K. Average K_a and standard deviations were determined by values obtained from binding curves generated for protons b, c, d, and e. [b] Ionization constants in water for diacids, pK_{a1} and pK_{a2} are listed. Unless otherwise noted, the data were taken from the *Dictionary of Organic Compounds*.[122] [c] Berger., W. E. Helv. Chim. Acta **1940**, *23*, 39−53. [d] Data in a 1:1 methanol/water mixture. Gumbley, S.J.; Stewart. R. *J. Chem. Soc. Perkin Trans. 2* **1984**, 529−531. [e] $K_a = 23 \pm 7$ M^{-1} in d-DMSO. [f] $K_a = 27 \pm 3$ when repeated as reverse titration (i.e., host added to guest acid solution). [g] No changes in spectrum were observed.

NMR Titrations of the Macrocyclic Hosts with Dicarboxylic Acids. Complexes **I**−**III** react with a number of aromatic or unsaturated dicarboxylic acids (Table 4), as observed by ^{1}H NMR spectroscopy. The gradual addition of a dicarboxylic acid to a CD_3CN solution of a macrocyclic complex causes significant changes in the ^{1}H NMR spectrum, similar to those shown in Figure 7. These shifts were reversible; the spectra of the original macrocycles were completely restored upon addition of triethylamine to the host−guest mixtures. Furthermore, titration of a dicarboxylic acid guest with a solution of the macrocyclic host gave rise to shifts of the diacid protons.

The protons of the pyridine receptor arms in hosts **I**−**III** experience the most significant and systematic shifts upon guest binding, although the protons of the macrocyclic platform also shift. In all cases (regardless of the system studied), protons on the receptor pyridine and ethyl arms shift downfield (with signals b, c, d showing the largest changes, $\Delta\delta = 0.60-0.80$ ppm downfield, and signal a corresponding to the pyridine proton adjacent to nitrogen shifts downfield by a smaller amount $\Delta\delta = 0.15$ ppm). Protons on the platform (v, p, q, r) mostly shift upfield to a lesser extent ($\Delta\delta = 0.01-0.20$ ppm). All changes in proton chemical shifts observed upon titrations of **I**−**III** with dicarboxylic acids are summarized in SI Table S19. Qualitatively very similar, although somewhat larger, shifts of the macrocyclic protons were also observed upon adding an excess of a strong acid (trifluoroacetic or triflic) to complexes **I**−**III**.

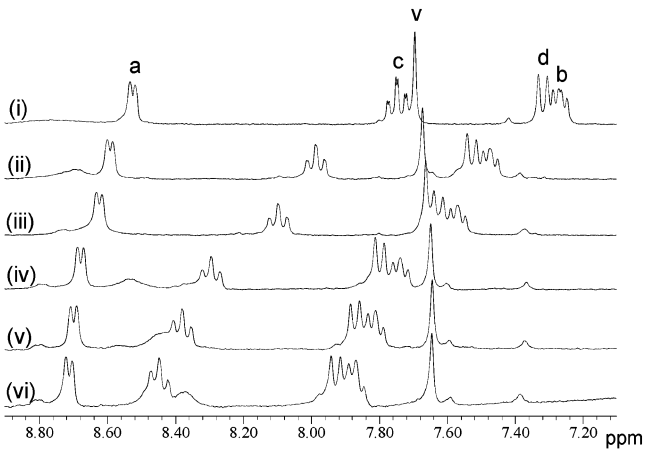

Figure 7. Downfield aromatic region of the ^{1}H NMR spectra of **I** (5.0 mM in CD_3CN) with standard additions of maleic acid (250 mM). Host **I** with 0 (i), 1.2 (ii), 2.0 (iii), 5.6 (iv), 10 (v), and 22 (vi) equiv of maleic acid added. See Figure 1 for atom labeling scheme.

Interestingly, instead of the two broad signals of protons f observed in room-temperature NMR spectrum of **III**, one well-resolved multiplet was obtained upon titrations of **III**

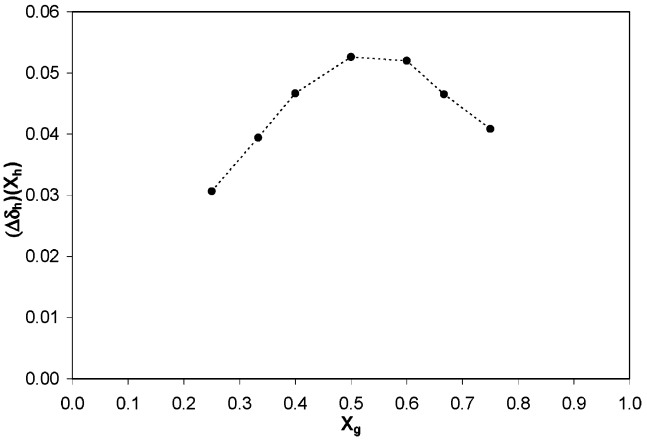

Figure 8. Job's plot analysis of proton c in determining stoichiometry of [14]NHEt2Py (**I**) with maleic acid in CD_3CN. The total concentration was held constant at 2.0 mM with X_g, mole fraction of guest; $\Delta\delta_h$, change in chemical shift of host proton; and X_h, mole fraction of host.

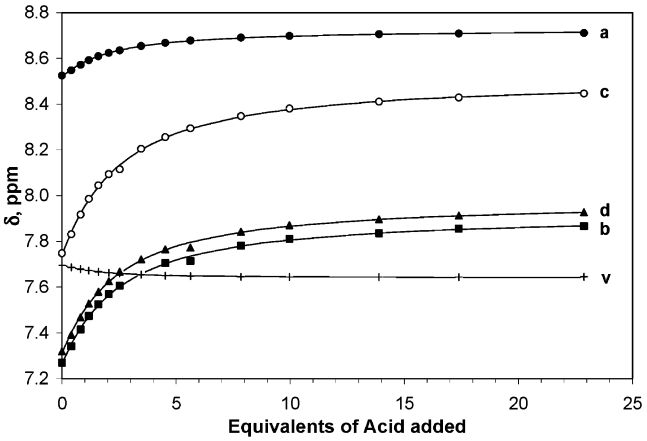

Figure 9. ^{1}H NMR titration binding curves of protons a (●), b (■), c (○), d (▲), and v (+) in the titration of 14NHEt2Py **(I)** with maleic acid. The data were fit considering formation of a 1:1 complex according to eq 1. See Figure 1 for atom labeling scheme.

with diacids. This behavior indicates that one conformation of the ethylpyridine arms is dominant in the host−guest adduct.

The pyridine signals (a, b, c, d) and the aliphatic protons from the ethylpyridine arms (protons e) were followed in quantitative studies of the dicarboxylate complexation with macrocycles **I**−**III**.

The stoichiometry of the macrocycle−dicarboxylic acid interaction was determined by the method of continuous variation.[78,79,81,82] A representative Job's plot for the system composed of the 14-membered macrocycle **I** and maleic acid is shown in Figure 8. For all dicarboxylic acids listed in Table 4, Job's plot analysis unambiguously showed the 1:1 stoichiometry of their complexes with the macrocyclic receptors **I**−**III**.

Association constants were determined from the binding curves (Figure 9) by nonlinear regression methods that gave excellent fits to a 1:1 model for the association between a host and a guest. For each host−guest pair, a series of binding curves were obtained. The calculated values of association constants were essentially independent of the position of the protons in the macrocycle. However, for regularity, binding constants using proton signals of the host (b, c, d, e), which showed the largest and most systematically reproducible shifts, are reported. Furthermore, for a system containing **I** and 3-nitrophthalic acid, the reverse titration was also performed, in which the acid was titrated with the macrocycle and the shifts of the aromatic protons of the acid were followed. The saturation curve yielded the equilibrium constant of 27 ± 3 M^{-1} that agrees very well with the equilibrium constant determined in the direct titration of the macrocycle with the diacid (20 ± 2 M^{-1}). The averaged results of NMR titrations are summarized in Table 4. Since the measured equilibrium constants for phthalic, 3-nitrophthalic, 5-nitroisophthalic, and maleic acids, K_{meas}, fall in the range from 10 to 10^4 M^{-1}, the NMR method is indeed adequate for accurate equilibrium measurements in the systems under investigation.[79]

The carboxylate binding constants were found to be sensitive to the nature of solvent; the binding of maleic acid with **II** was almost an order of magnitude weaker in DMSO than it was in acetonitrile (Table 4).

For several dicarboxylic acids listed in Table 4, very small shifts of the host protons were observed (ca. 0.01−0.08 ppm) and the titration curves did not approach saturation. In the cases of iso- and terephthalic acids, this behavior could be attributed to extremely low solubility of these acids in acetonitrile. 2-Nitroterephthalic acid, however, was sufficiently soluble, and fumaric acid was somewhat soluble in CD_3CN, and yet very weak binding was observed. We also found that aliphatic dicarboxylic acids (succinic, glutaric, and sebacic) did not interact strongly with the macrocyclic receptors **I**−**III** (although malonic acid caused some shifts in the NMR spectra of the macrocyclic hosts).

Important control experiments were performed with monocarboxylic acids. The strong trifluoroacetic acid interacted with macrocyclic complexes **I**−**III**, causing NMR shifts similar to those observed for dicarboxylate binding. In this case, titration curves had a clear sharp inflection point at a 2:1 molar ratio of acid−macrocycle, indicating a strong interaction with a 2:1 stoichiometry. Similar behavior was observed also for titrations of **I**−**III** with triflic acid. In contrast, weaker monocarboxylic acids did not cause any spectral changes in the proton NMR spectra of the macrocycles **I**−**III** (this behavior was found for benzoic acid), or gave rise to minor shifts of the proton NMR signals upon titration of **I**−**III** with *o*- or *p*-nitrobenzoic acids. No interaction was detected between the macrocyclic receptors **I**−**III** and nitrobenzene.

To summarize, relatively strong diacids (pK_{a1} from ca. 1.5 to ca. 3, Table 4) with 1,2- or 1,3-positioned carboxylate groups bind to the macrocyclic ditopic receptors **I**−**III**. The corresponding monoacids do not cause substantial shifts in the NMR spectra of **I**−**III**.

NOESY of a Host−Guest Adduct. The high binding affinity of dicarboxylic acids with the ditopic macrocyclic hosts, as opposed to very low binding of their monofunctional counterparts, suggests that a two-point interaction is important for strong host−guest complexation. To shed light on the binding mode of dicarboxylates, the 2D NOESY experi-

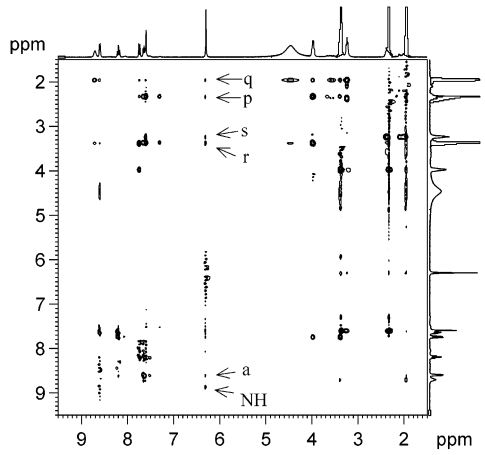

Figure 10. NOESY spectrum of 20 mM solution of 1:1 maleic acid and **II** in CD_3CN. Letters denote NOE cross signals for maleic acid guest (CH protons) and host **II**. See Figure 1 for atom labeling scheme.

Table 5. Relative Intensities of NOESY Cross-Peaks and Calculated Distances in **II**−Maleic Acid System[a]

correlated protons	intensity (arbitrary units) (F2, F1 domain)	estimated distance (Å)[c] (F2, F1 domain)
Selected Intramacrocyclic (Host−Host) Correlations		
a−b	38.8, 63.5	2.43, 2.24[b]
b−c	40.4, 52.3	2.42, 2.32[b]
c−d	54.9, 53.9	2.30, 2.30[b]
Macrocycle−Maleic Acid (Host−Guest) Correlations		
m−q	7.01, 6.90	3.24, 3.25
m−p	7.94, 8.66	3.17, 3.12
m−s	7.01, 6.16	3.24, 3.31
m−r	10.2, 11.7	3.04, 2.97
m−a	2.77, −	3.78, −
m−NH (complex shifted)	7.01, −	3.24, −

[a] 20 mM 1:1 maleic acid−**II** solution in CD_3CN at 25 °C. See Figure 1 for atom labeling scheme. [b] Estimated from the crystal structure of the macrocyclic host **II** (a−b = 2.298, b−c = 2.343, c−d = 2.370 Å). [c] Calculated from the relative intensities of the host−host and host−guest cross-peaks, using the X-ray distances for host−host proton pairs and a $1/r^6$ dependence for the intensities of the NOEs.

ment was performed on the **II**−maleic acid system. In this system, sharp, well-resolved signals were observed in 1D proton spectra of the host and of the host−guest mixtures. The guest has only one kind of CH protons ($\delta = 6.3$ ppm) that are well separated from the signals of the host. A reasonably strong binding ($K = 159\ M^{-1}$) ensures that a high fraction of the host−guest adduct is present in the sample. The 2D NOESY spectrum was acquired from a 20 mM solution of a 1:1 mixture of **II** with maleic acid in degassed CD_3CN at room temperature. Under these conditions, about 60% of the macrocycle **II** was present in the form of its complex with the guest. The spectrum depicted in Figure 10 clearly shows a number of cross-peaks between the macrocyclic protons and several additional cross-peaks that correspond to the interactions between the vinyl protons of maleic acid and the protons of the macrocyclic host (Table 5). Although these cross-peaks are relatively weak, they are seen in both domains of the unsymmetrized spectrum, and their intensity does not depend on the mixing time of NOESY experiments (500 or 1000 ms). Four cross-peaks were observed in both domains that correspond to the both methyl groups (p, q), and methylenes (r, s) on the saturated ethyl and propyl portions of the platform. Additionally, two very weak cross-peaks are seen in the aromatic region, which corresponds to a and the NH proton. The NH signal is shifted slightly downfield as compared to the pure host **III** due to an interaction with maleic acid, the same behavior that was also observed in titration experiments. The overall picture reflects the formation of a host−guest adduct between macrocycle **II** and maleic acid and is quite similar to the spectra obtained for other similar host−guest systems.[111−113] No host−guest cross-peaks were registered in dilute solutions (5 mM) in nuclear Overhauser effect (NOE) difference experiments.

Other than the cross-peaks between the host−guest complex, there are additional cross-peaks related to the platform alone. Strong correlations were observed between p−v, p−f, q−s, s−t, r−v, e−f, and medium cross-peaks correspond to q−NH, e−d, f−d (weaker than e−d), a−b, b−c, and c−d. Several of these cross-peaks (Table 5) were used for an "internal calibration" of NOE intensities. For these pairs of protons, the possible changes in the conformation of the macrocyclic host upon complexation would not cause substantial differences in H−H distances, and the X-ray data for the host itself provide a reasonably accurate estimate of the H−H separations. Considering that the NOE intensities are inversely proportional to the sixth power of the distance,[114] the intensities of the cross-peaks with known H−H distances could be used in estimating interatomic distances between the correlated protons in the host−guest assembly: $I_{st}/(r_{st})^6 = I_{hg}/(r_{hg})^6$ (where st corresponds to the standard H−H pairs within the macrocyclic host and hg corresponds to H−H correlations between the protons of a host and a guest). The data suggest that the vinyl protons of maleic acid are ca. 3−3.5 Å from the pyridine receptor arms and from the macrocyclic platform, in agreement with a 1:1 inclusion binding mode where the acid is coordinated to both $NHCH_2$-CH_2Py fragments, being positioned above the metallomacrocyclic framework. In the absence of encapsulation of diacid, one would not expect substantial correlation between the maleic acid protons and the saturated chelate rings of the cyclidene platform. The flexibility of the receptor "arms" and the dynamic nature of complexation−decomplexation process does not allow us to quantitatively model the structure of a host−guest adduct.

Discussion

A series of metallomacrocyclic ditopic receptors for dicarboxylic acids were prepared by attaching aminoethylpyridine groups to the cyclidene platforms. The major

(111) Yanagihara, R.; Katoh, M.; Hanyuu, M.; Miyazawa, T.; Yamada, T. *J. Chem. Soc., Perkin Trans. 2* **2000**, 551−556.
(112) Mizuno, Y.; Aida, T.; Yamaguchi, K. *J. Am. Chem. Soc.* **2000**, *122*, 5278−5285.
(113) Goshe, A.; Steele, I. M.; Bosnich, B. *J. Am. Chem. Soc.* **2003**, *125*, 444−451.
(114) Silverstein, R. M.; Bassler, G. C.; Morill, T. C. *Spectrometric Identification of organic compounds*, 5th ed.; Wiley: New York, 1991.

difference in chemical structures of the three complexes (**I**−**III**) is the size of the macrocyclic ring. In complete agreement with the literature,[53] the local environment of the nickel(II) central metal ions did not change dramatically upon an increase in the ring size from the 14-membered to the 16-membered ring. The nickel(II) ions remained four-coordinate, low-spin in all three complexes **I**−**III**. The X-ray data show that the average Ni−N bond distance increases slightly in the series **I** < **II** < **III.** Consequently, all three macrocycles with alternating saturated and unsaturated chelate rings (5656, 5666, and 6666 chelate ring sequences) accommodate the low-spin nickel(II) reasonably well. The nonsymmetric 15-membered complex **II**, however, displays more substantial distortion of the NiN_4 fragment, as can be seen in significant deviations of the metal coordination sphere from planarity (the nickel ion is displaced by 0.1085 Å). The UV−vis spectra demonstrate systematic, but not dramatic, changes in the electronic structure of nickel(II) within the three macrocycles (an increase in d−d orbital energy separation for a larger ring). Interestingly, the ring size effect is less pronounced for the d−d transitions in the 15-membered macrocycle **II,** possibly due to distortions in the nickel(II) coordination sphere in this complex.

The long-range effects of the macrocyclic ring size on the overall molecular shape of cyclidenes are profound; the 14-membered complexes are planar, the 16-membered ones fold into a saddle-shaped conformation, and the 15-membered complexes can exist in both planar and cleftlike conformations.[53,54,107] The high degree of conjugation in the unsaturated chelate rings accounts for the fact that the entire "wing" moves in response to the changing conformation of the saturated chelate rings of different sizes. As a result, the separation and mutual orientation of the substituents appended at the periphery of cyclidenes are highly sensitive to the size and geometry of the macrocycle. We expected to observe this structural effect in a series of cyclidenes bearing receptor groups at the periphery and to explore the influence of the overall molecular shape on substrate encapsulation between the appended receptor arms.

Our crystallographic data confirm the expected geometries of the 14- and 16-membered macrocycles **I** and **III**, planar and saddle-shaped, respectively. The 15-membered complex **II** was found to exist in the "open", nearly planar geometry in the solid sate, resembling the overall molecular shape of the 14-membered complex **I** (Figures 4−6). Unlike the 14-membered complex **I**, in which the two unsaturated wings are almost coplanar with the NiN_4 fragment, the 15-membered **II** has the unsaturated wings tilted in opposite directions. It is thus likely that an alternative saddle-shaped conformation of **II** (with both unsaturated wings facing the same direction) is close in energy to the structure determined by X-ray diffraction. This assumption is based on several literature reports that documented both Z-shaped and U-shaped geometries of the 15-membered cyclidenes and their precursors.[53,54] Furthermore, in bridged 15-membered cyclidenes, the macrocyclic platform is invariably cleftlike and has a cavity size comparable to that of the corresponding 16-membered complexes.[53] In contrast, the 14-membered

Chart 2. Inclusion Binding Mode of Dicarboxylic Acids by **I**−**III**

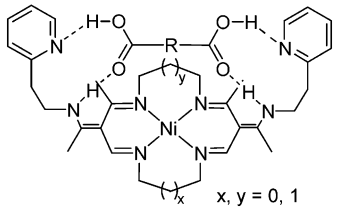

platform, with a large distance between the ends of the "open" macrocycle, could only be bridged with a long C_{12} aliphatic chain that was able to span it.[74] Molecular mechanics and molecular dynamics calculations also support the accessibility of a saddle-shaped geometry in 15-membered cyclidenes and related molecules and a predominantly planar conformation of the 14-membered complexes.[55,56,115]

The ethylpyridine arms were expected to be the most flexible parts of the complexes **I**−**III**. This assumption was confirmed by both X-ray crystallography and NMR. Two independent molecules that differ in orientation of the ethylpyridine arms coexist in the unit cell of **III** (Figure 6). Moreover, in solution, the variable-temperature proton NMR of **III** demonstrates intermediate exchange at room temperature and rapid exchange at 65 °C (Figure 2). Consequently, the change in orientation of the ethylpyridine groups in this complex occurs on the NMR time scale at room temperature, reflecting rotational barriers about the N3−C5 and N7−C18 bonds that are between the values for a regular single and a regular double bond. The flexibility of the aliphatic linkers that were used to attach receptor groups to the cyclidene platforms allows for substantial adjustments of the host geometry to the geometric requirements of the encapsulated guests.

All three complexes were found to interact with carboxylic acids, as evidenced by substantial changes in the proton NMR spectra of both the hosts and the guests. Upon the addition of dicarboxylic acids, the nickel(II) complexes remain low spin, and the UV−vis spectra do not change significantly. These results indicate the lack of carboxylate coordination to the nickel(II) centers. The carboxylic acid binding can be attributed to the partial protonation and hydrogen bonding with the ethylpyridine fragment and an exocyclic NH group (see Chart 2). The exocyclic NH group of the cyclidenes is conjugated with the unsaturated part of the platform and has an amide-like character. Indeed, this group is known to undergo deprotonation upon addition of strong bases.[72,116,117] Amidopyridine fragments are well-known receptors for carboxylic acids, in which the pyridine nitrogen acts as an H-bond acceptor (or a proton acceptor) and an NH group acts as a hydrogen-bond donor.[5] Hydrogen bonding in the host−guest complexes between dicarboxylic acids and macrocycles **I**−**III** is confirmed by NMR; the dicarboxylic acid-induced NMR shifts of the protons in the ethylpyridine

(115) Lin, W.-K.; Alcock, N. W.; Busch, D. H. *J. Am. Chem. Soc.* **1991**, *113*, 7603−7608.
(116) Hipp, C. J.; Corfield, P. W. R.; Mokren, J. D.; Busch, D. H. *J. Am. Chem. Soc.* **1973**, *95*, 4465−4466.
(117) Goldsby, K. A.; Jircitano, A. J.; Nosco, D. L.; Stevens, J. C.; Busch, D. H. *Inorg. Chem.* **1990**, *29*, 2523−2527.

fragments are somewhat smaller than the shifts due to full protonation of pyridine nitrogens in **I**−**III** with strong acid (SI Table S19). Not surprisingly, pyridine-appended receptor **II** does not bind dicarboxylic acids (e.g., maleic acid) as strongly as was reported for an analogous cyclidene host bearing polyamine macrocyclic receptor arms under the same experimental conditions (DMSO, 25 °C).[71] The polyamine (cyclene) receptor is a much stronger base than the pyridine, and it has more possibilities for hydrogen bonding and electrostatic interactions with carboxylate guests. However, the strong basic properties of cyclene had a drawback: the cyclene-containing molecular tweezer suffered from base-induced self-decomposition in polar solvents (such as water, methanol, or acetonitrile). The weaker basicity of the pyridine receptors allowed for the improved stability of hosts **I**−**III**.

Relatively strong 1:1 complexation between complexes **I**−**III** and dicarboxylic acids, and the lack thereof in the case of monocarboxylic acids, suggests that both ethylpyridine receptor arms in the macrocyclic hosts participate, in a cooperative manner, in the encapsulation of dicarboxylate guests (Chart 2). One can argue that the higher acidity of aromatic dicarboxylic acids as compared to benzoic acid would increase their interaction with ethylpyridine arms. However, nitrobenzoic acids are almost as strong as their difunctional counterparts (Table 4) and yet 2- and 4-nitrobenzoic acids do not bind to the macrocycles **I**−**III** to an appreciable extent. It can be concluded that the presence of two carboxylic groups in the guest molecule is crucial for substantial host−guest binding in our systems. Additional evidence in favor of guest encapsulation between the two receptor arms comes from the analysis of the NMR data. The NOESY spectrum for the maleic acid−**II** system clearly shows through-space correlations between the guest protons and the protons from the macrocyclic platform as well as the protons of the pyridine arms. The 3.0−3.5 Å distances between the maleic acid and the macrocycle corresponds to an inclusion binding mode. In the case of the 16-membered complex **III**, difunctional guest binding inhibits the flipping of the receptor arms between "outside-the-cavity" to "inside-the-cavity" orientations (i.e., the signal that corresponds to the "inside-the-cavity" orientation of the arm, Figures 2 and 6, disappears upon addition of the diacid). An alternative supramolecular motif that could lead to a strictly 1:1 stoichiometry of the macrocycle−dicarboxylic acid adducts, a linear oligomer with intermolecular binding of the dicarboxylate, was previously found in a number of solid-state structures[118−121] but is unlikely to dominate in dilute solutions. The stability of the oligomers should depend on the overall concentration of host−guest solution, a behavior that was not observed in our systems.

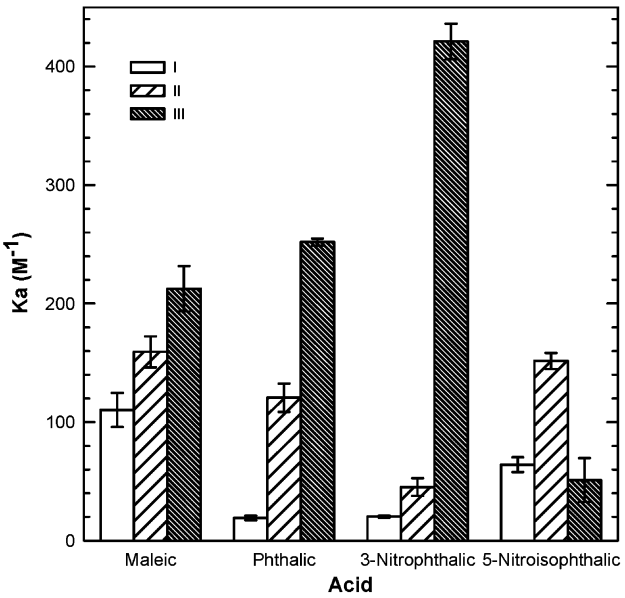

Figure 11. Graphical comparison of binding constants for four dicarboxylic acids and compounds **I**−**III**.

The proposed intramolecular inclusion binding mode (Chart 2) implies that shape complementarity between the host (receptors **I**−**III**) and the guest (dicarboxylic acid) is beneficial for high affinity binding. Analysis of the binding constants (Table 4, Figure 11) shows that the binding strength depends on the structures of both the host and the guest. While acidity of the guest clearly is a factor that influences the binding strength, the separation between the two carboxylate groups and the distance between them also play an important (and sometimes decisive) role in binding affinity. While 1,2- and 1,3-aromatic and *cis*-1,2-unsaturated diacids bind reasonably well (with the affinity constants ranging from 20 to 400 in acetonitrile), the 1,4-aromatic and *trans*-1,2-unsaturated diacids show very small, if any, interaction with the macrocyclic hosts **I**−**III**. In some cases (e.g., with terephthalic, or to some extent, fumaric acid), the limited solubility of diacids partially accounts for small NMR shifts and the lack of saturation on the binding curves. In some other cases, however, the diacids have sufficient solubility and still demonstrate only weak binding to the macrocyclic hosts. A good example is 2-nitroterephthalic acid, which has sufficient solubility in acetonitrile and ionization constants comparable to or exceeding the values for other isomers of nitrophthalic acids (Table 4). The unfavorable orientation of the two carboxylic groups prevents a strong interaction between this acid and the macrocycles.

The macrocyclic ring size (and, consequently, the shape of the host molecule) has a pronounced effect on the diacid binding affinity (Figure 11). For all acids that bind relatively strongly, the planar 14-membered macrocycle **I** has the weakest binding affinity for diacid guests. In most cases, the saddle-shaped 16-membered macrocycle **III** is the best receptor. The 15-membered complex **II**, which can adopt either an almost planar, or a saddle-shaped conformation, usually displays an intermediate binding affinity. Interestingly, this trend holds for all 1,2-aromatic or cis-unsaturated diacids investigated in this work. However, the aromatic 1,3-

(118) Min, K. S.; Suh, M. P. *Eur. J. Inorg. Chem.* **2001**, 449−455.
(119) Garcia-Tellado, F.; Geib, S. J.; Goswami, S.; Hamilton, A. D. *J. Am. Chem. Soc.* **1991**, *113*, 9265−9269.
(120) Yang, J.; Fan, E.; Geib, S. J.; Hamilton, A. D. *J. Am. Chem. Soc.* **1993**, *115*, 5314−5315.
(121) Kimura, E.; Ikeda, T.; Shionoya, M.; Shiro, M. *Angew. Chem., Int. Ed. Engl.* **1995**, *34*, 663−664.
(122) Chapman & Hall/CRC Chemical Dictionaries on CD-ROM (version 10: 1) 10: 1 (based on 6th print edition) *CDROM resource*; Chapman and Hall, CRC Press: Boca Raton, FL, 2002.

diacid (5-nitroisophthalic acid) has a 3-fold higher binding affinity to **II** than it has to the saddle-shaped host **III**. Apparently, the average separation between the two pyridine receptor centers in **II** is greater than the distance between the pyridine receptors in **III**. This greater separation is unfavorable for the strong binding of 1,2-diacids but becomes favorable for the corresponding 1,3-diacid. It can be concluded that the molecular shape of the cyclidene platform significantly influences the guest binding affinity of ditopic hosts and in some cases even changes the selectivity of the hosts. This molecular shape effect is observed in systems that have flexible appended receptor arms, and this flexibility is beneficial for an "induced-fit" guest binding. Indeed, the orientation of the pyridine arms in the solid macrocycles **I**−**III** did not show substantial preorganization for the dicarboxylate encapsulation. It can be assumed that the host−guest interaction repositioned the ethylpyridine groups in order to accomplish a good fit between the host and the guest. In the case of the 14-membered platform that cannot fold, the conformational flexibility of the receptor arms was necessary to accommodate the bifunctional guests. For the 15-membered complex, it can be hypothesized that the platform adopted a saddle-shaped conformation in the host−guest complex that is favorable for guest encapsulation. This cleftlike confirmation of the platform already existed in the solid state of the 16-membered complex. The flexibility of the receptors allowed for moderate selectivity of host−guest interactions with **I**−**III**. The effects of molecular shape and macrocycle-dependent size and shape selectivity may be even more pronounced in systems with rigid receptor groups directly attached to the cyclidene platforms. The exploration of such systems is being pursued.

Conclusions

Metal binding within cyclidene platforms of different macrocyclic ring sizes indirectly effects the molecular shape and the mutual orientation of two receptor sites appended on the periphery of the cyclidenes. The ethylpyridine-containing cyclidenes **I**−**III** were found to bind dicarboxylic acids between the two receptor cites with affinity constants approaching 4×10^2 M^{-1} in acetonitrile. Consequently, ditopic cyclidenes act as molecular tweezers with respect to the dicarboxylic acid guests. The binding affinity of the hosts depends dramatically on the molecular shape; the planar macrocycle is a substantially poorer host than its saddle-shaped counterpart. The selectivity of the hosts with respect to dicarboxylic acids also depends on the molecular shape; 1,2-diacids display the highest affinity for the saddle-shaped 16-membered cycliene host **III**, while an aromatic 1,3-diacid has the highest binding affinity for the more flexible 15-membered molecular tweezer **II**.

Acknowledgment. Financial support was provided by Tufts University (startup funds and FRAC) and the NSF. The CCD-based X-ray diffractometer at Tufts University was purchased through Air Force DURIP Grant F49620-01-1-0242. The CCD-based X-ray diffractometer at Harvard University was purchased through NIH grant (1S10RR11937-01). The NMR facility in the Chemistry Department at Tufts University is supported by NSF Grant CHE-9723772. J.S.D. would like to thank his wife Greta for her support and the Rybak-Akimova lab for helpful discussions.

Supporting Information Available: Tables of crystallographic solution data, atomic coordinates and bond lengths and angles, displacement parameters, hydrogen coordinates, and torsional angles; figures depicting hydrogen bonding of NH to PF_6^- anions and $\pi-\pi$ stacking interactions between the pyridine rings and the unsaturated portions of the cyclidenes; table of total chemical shift change observed during titration experiments; and elucidation of ^1H and ^{13}C signal assignments by 2D NMR techniques: **I** (NOESY), **II** (COSY, HMQC, HMBC), and **III** (COSY, HMQC, NOESY) in PDF format. X-ray crystallographic files in CIF format for **I**, **II**, and **III**. This material is available free of charge via the Internet at http://pubs.acs.org

IC0345572